

# Implantable Energy-Harvesting Devices

Bojing Shi, Zhou Li,\* and Yubo Fan\*

The sustainable operation of implanted medical devices is essential for healthcare applications. However, limited battery capacity is a key challenge for most implantable medical electronics (IMEs). The human body abounds with mechanical and chemical energy, such as the heartbeat, breathing, blood circulation, and the oxidation–reduction of glucose. Harvesting energy from the human body is a possible approach for powering IMEs. Many new methods for developing *in vivo* energy harvesters (IVEHs) have been proposed for powering IMEs. In this context energy harvesters based on the piezoelectric effect, triboelectric effect, automatic wristwatch devices, biofuel cells, endocochlear potential, and light, with an emphasis on fabrication, energy output, power management, durability, animal experiments, evaluation criteria, and typical applications are discussed. Importantly, the IVEHs that are discussed, are actually implanted into living things. Future challenges and perspectives are also highlighted.

## 1. Introduction

Most current implantable medical electronics (IMEs), including cardiac pacemakers, defibrillators, deep brain stimulators, and cochlear implants are powered by batteries. Owing to the limited capacity of batteries and size restrictions, the lifetime

Dr. B. Shi, Prof. Y. Fan  
Beijing Advanced Innovation Center for Biomedical Engineering  
School of Biological Science and Medical Engineering  
Beihang University  
Beijing 100083, China  
E-mail: yubofan@buaa.edu.cn

Dr. B. Shi, Prof. Z. Li  
CAS Center for Excellence in Nanoscience  
Beijing Key Laboratory of Micro-nano Energy and Sensor  
Beijing Institute of Nanoenergy and Nanosystems  
Chinese Academy of Sciences  
Beijing 100083, China  
E-mail: zli@binn.cas.cn

Dr. B. Shi, Prof. Y. Fan  
Key Laboratory of Biomechanics and Mechanobiology  
Beihang University  
Ministry of Education  
Beijing 100083, China

Prof. Z. Li  
School of Nanoscience and Technology  
University of Chinese Academy of Sciences  
Beijing 100049, China

Prof. Z. Li  
Center on Nanoenergy Research  
School of Physical Science and Technology  
Guangxi University  
Nanning 530004, China

 The ORCID identification number(s) for the author(s) of this article can be found under <https://doi.org/10.1002/adma.201801511>.

DOI: 10.1002/adma.201801511

of a cardiac pacemaker, for example, is about 7–10 years, and 3–5 years for a deep brain stimulator.<sup>[1]</sup> The battery contributes most of the weight and size of IMEs. Thus, efforts to reduce the weight and size of IMEs while improving the battery life has attracted a great deal of attention recently.<sup>[2]</sup>

The human body produces abundant kinetic and biochemical energy. For instance, the cardiac output power is about 1.4 W.<sup>[3]</sup> If a small fraction of the biomechanical energy released during cardiac contraction and relaxation could be harvested and used to power a cardiac pacemaker, it may represent a promising alternative to solve the problems of limited battery life. In addition to energy from heartbeats, lung motion and the

systolic/diastolic deformations of the ascending aorta are also possible energy sources in living organisms. Recently, piezoelectric materials have been utilized for harvesting heartbeat and respiratory biomechanical energy in rats, cows, pigs, and others.<sup>[4–6]</sup> Triboelectrification between two materials in contact is also suitable for harvesting mechanical energy.<sup>[7]</sup> Triboelectric *in vivo* energy harvesters (IVEHs) have already been used to collect biomechanical energy from the heartbeat and respiration of rats and pigs.<sup>[8,9]</sup> Other approaches for harvesting *in vivo* biomechanical energy include the use of an automatic-wristwatch IVEH to utilize the heartbeats of large mammals,<sup>[10–12]</sup> or using optical energy via solar cells, which have already been implanted into rats, rabbits, and pigs.<sup>[13–15]</sup>

Biochemical energy harvesting is a type of energy conversion that utilizes *in vivo* chemical energy. Glucose is an abundant fuel in living things. The oxidation of glucose and the reduction of oxygen can occur at enzyme-modified electrodes. One of the primary shortcomings of biofuel IVEHs is the insufficient output voltage. To our knowledge, the required voltage of most of IMEs is 2–3 V, but most biofuel IVEHs cannot satisfy this requirement. The typical output voltage of biofuel cells is only 0.5 V, which is thermodynamically limited by the redox potentials of oxygen and the biofuel.<sup>[16]</sup> Some approaches have been demonstrated to increase the output voltage, including connecting several biofuel cells in series,<sup>[17,18]</sup> or storing electrical energy in capacitors or mediators for releasing short pulses.<sup>[19,20]</sup> Endocochlear potential (EP) is another type of *in vivo* biochemical energy source at the cochlear endolymphatic spaces, which has been investigated in guinea pigs.<sup>[21]</sup>

Besides acting as energy conversion devices, IVEHs can also be used as biomedical sensors. For example, an implantable triboelectric active sensor (iTEAS) fixed to the pericardium of a pig can be used for monitoring heart and respiratory rates,

as well as detecting life-threatening arrhythmia.<sup>[22]</sup> A flexible piezoelectric energy harvester affixed to a porcine heart between the left ventricular apex and right ventricle can be used for monitoring cardiac function.<sup>[8]</sup> Furthermore, the energy harvesters based on piezoelectric and triboelectric nanogenerators can be used for stimulation of living cell, tissue and organs, which provide potential applications in the fields of promoting neuronal differentiation of stem cells, facilitating neuronal tissue regeneration, and stimulating heart.<sup>[23,24]</sup>

The purpose of this review is to classify and summarize all of the realized *in vivo* energy harvesting devices that have actually been implanted into living things. Physical methods, the piezoelectric or triboelectric effect, as well as the use of nanogenerators and automatic wristwatches, can convert kinetic energy into electricity. Chemical methods, including biofuel cells that use glucose in living organisms, or that take advantage of the endocochlear potential maintained by the inner ear that creates a battery-like electrochemical gradient, can be used for powering electronic devices. Solar cells cannot harvest *in vivo* bioenergy directly, but instead collect light energy from the ambient environment to support implanted devices. These *in vivo* energy harvesting methods may provide solutions for battery-free and self-powered IMEs. We will discuss IVEHs with regard to their fabrication, energy output, power management, durability, animal experiments, evaluation criteria, and typical applications. In addition, future challenges and perspectives are also highlighted in this review.

## 2. Types

### 2.1. Piezoelectric Devices

Piezoelectric materials are capable of mechanical-to-electrical energy conversion. For instance, ZnO has a wurtzite structure, which includes a noncentral symmetry. When an external force is applied, positive and negative charged surfaces are generated, called polar surfaces. The piezoelectric potential created by these polar surfaces can be used to drive electrons in an external circuit, realizing the conversion of mechanical energy into electricity. To date, the piezoelectric materials primarily used for IVEHs include ZnO, lead zirconate titanate (PZT), polyvinylidene fluoride (PVDF), and barium titanate (BaTiO<sub>3</sub>).

In 2010, Li et al.<sup>[4]</sup> demonstrated a single wire generator (SWG) based on ZnO, which was implanted into a live rat to harvest the energy generated by its breathing and heartbeat (**Figure 1a**). The diameters of the ZnO wires were 100–800 nm, and their lengths were 100–500  $\mu\text{m}$ . The combination of the piezoelectric effect and the gating effect of the Schottky<sup>[25]</sup> contact at the interfaces caused the SWG to act as a “charging pump” that drove electron motion, generating an alternating current in the external circuit. The open-circuit voltage ( $V_{oc}$ ) and short-circuit current ( $I_{sc}$ ) were 1 mV and 1 pA, respectively, when implanted on ventral side of the diaphragm, and 3 mV and 30 pA when tightly fixed to the heart surface. The group applied AC nanogenerators to the *in vivo* harvesting of biomechanical energy, which represents the first successful attempt to convert the active biomechanical energy from normal breathing and heartbeats into electricity.



**Bojing Shi** received his Ph.D. from University of Chinese Academy of Sciences in 2017, and B.E. degree from University of Electronic Science and Technology of China in 2012. He is currently doing postdoctoral research at Beijing Advanced Innovation Centre for Biomedical Engineering, Beihang University. His research work is focusing on nanogenerators, implantable energy devices, and self-powered biosensors and systems.



**Zhou Li** received his Ph.D. from Peking University in Department of Biomedical Engineering in 2010, and Medical Degree from Wuhan University in Medical School, 2004. He joined School of Biological Science and Medical Engineering of Beihang University in 2010 as an associate professor. Currently, he is a professor in Beijing Institute of Nanoenergy and Nanosystems, CAS. His research interests include nanogenerators, *in vivo* energy harvesters, and self-powered medical devices, biosensors.



**Yubo Fan** is the Dean of School of Biological Science and Medical Engineering, Director of Key Laboratory for Biomechanics and Mechanobiology of Ministry of Education of Beihang University, Director of National Research Centre for Rehabilitation Technical Aids of China. He specializes in biomechanics, mechanobiology, and biomaterials.

In 2014, Dagdeviren et al.<sup>[5]</sup> reported a flexible PZT type of IVEHs. Ten PZT ribbons, each with a size of 2.02 mm  $\times$  100  $\mu\text{m}$   $\times$  500 nm, were connected in parallel to form a group. Then, 12 groups were connected in series to form the key functional element of the IVEH. Furthermore, the researchers integrated PZT energy-harvesting elements, a rectifier, and rechargeable microbattery, on a flexible polyimide (PI) substrate. They placed the entire energy harvesting system on a bovine heart, lung, or diaphragm to convert the mechanical energy of the contractions and relaxations of those organs into electricity.

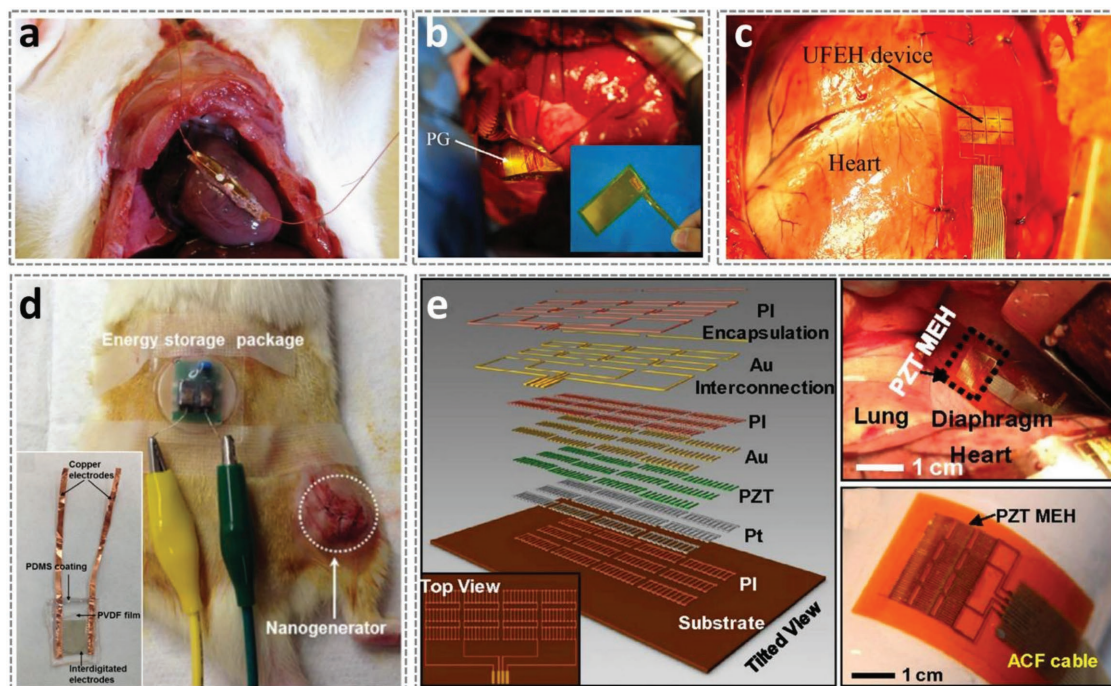


**Figure 1.** a) The SWG attached to a live rat's heart. Reproduced with permission.<sup>[4]</sup> Copyright 2010, Wiley-VCH. b) PVDF-based PG was implanted to wrap around the ascending aorta of a porcine. Reproduced with permission.<sup>[26]</sup> Copyright 2015, Elsevier. c) PZT-based IVEH was implanted to harvest heart beat energy of swine. Reproduced with permission.<sup>[6]</sup> Copyright 2015, Springer Nature. d) PVDF-based nanogenerator was implanted between the epithelial and muscle layer in the thigh region of a rat to harvest mechanical energy from movement of rodent muscle. Reproduced with permission.<sup>[28]</sup> Copyright 2016, Elsevier. e) PZT mechanical energy harvester (MEH) was implanted to harvest energy from movements of the heart, lung, and diaphragm of a bovine heart. Reproduced with permission.<sup>[5]</sup> Copyright 2014, National Academy of Sciences.

The output properties of this type of IVEH indicated that the placement and orientation on organs, as well as the conditions of the organs, such as heart size, rate, and contractile force, can affect the output voltage. To demonstrate mechanical and electrical stability over a long duration, the researchers exposed the device to over 20 million bending/unbending cycles in moist and hydrogel environments (Figure 1e).

In 2015, Zhang et al.<sup>[26]</sup> proposed a flexible implantable piezoelectric nanogenerator (PENG) based on a PVDF film with a size of 2.5 cm × 5.6 cm × 200 μm (Figure 1b). They implanted the device wrapped around the ascending aorta of a pig and harvested biomechanical energy from the pulsation of the vessel. The *in vivo* results showed that typical  $V_{oc}$  and  $I_{sc}$  values were 1.5 V and 300 nA, respectively, at a blood pressure of 160/105 mmHg and a heart rate of 120 bpm. The tightness of the wrapping around the ascending aorta markedly impacted the output, and optimization of the wrapping tension is a key point for obtaining high output levels from this implantable PENG.

Lu et al.<sup>[6]</sup> reported an ultraflexible PZT ceramic-based piezoelectric device used to harvest biomechanical energy from heart motions, which was implanted in pigs under different conditions, such as with an open or closed chest, or awake or under anesthesia (Figure 1c). The peak-to-peak voltage was up to 3 V when the device was fixed between the right ventricle and the left ventricular apex after sternal closure. This output voltage was approximately the same as the required value for biomedical implants, about 2.4–2.8 V for a commercial cardiac pacemaker, for example. Their study demonstrated that the output properties of the PZT device were related to the implantation site.

In 2016, Cheng et al.<sup>[27]</sup> demonstrated an IVEH based on a piezoelectric thin film (PETF) that was implanted to wrap around the ascending aorta of a Yorkshire pig to scavenge pulsation energy. The device also measured the blood pressure at the same time. In this way, the researchers established a self-powered implantable device that monitored blood pressure with an *in vivo* maximal instantaneous power of 40 nW. Yu et al.<sup>[28]</sup> reported a mesoporous PVDF film-based implantable PENG, which can harvest mechanical energy from the gentle movement of rodent muscles (Figure 1d). They implanted the device under the skin of the right leg of a living rat. About 200 mV ( $V_{oc}$ ) was generated by the movement of the muscles. Moreover, they tested the stability of the PENG after five days of *in vivo* operation, corresponding to 151.2 million mechanical deformations.

In 2017, Jeong et al.<sup>[29]</sup> used aerosol deposition and a laser lift-off processing method to fabricate an IVEH based on LiNbO<sub>3</sub>-doped (K,Na)NbO<sub>3</sub>(KNN) thin films. They implanted the device into a porcine chest, and about 5 V and 700 nA were generated by the motion from the heartbeat. Kim et al.<sup>[30]</sup> presented an *in vivo* piezoelectric energy harvester based on high-performance single-crystalline (1-x)Pb(Mg<sub>1/3</sub>Nb<sub>2/3</sub>)O<sub>3</sub>-(x)Pb(Zr,Ti)O<sub>3</sub> (PMN-PZT), which generated a  $V_{oc}$  of 17.8 V and an  $I_{sc}$  of 1.74 μA from porcine heartbeats. In addition, the PMN-PZT energy harvester was used to make a self-powered wireless communication system. Wang et al.<sup>[31]</sup> fabricated poly(vinylidene fluoride-trifluoroethylene) (P(VDF-TrFE)) nanofiber scaffolds (NFSs) using optimized electrospinning, and used them to harvest the kinetic energy of leg motion. This system was

implanted under the skin of the leg of a Sprague–Dawley (SD) rat. The *in vivo*  $V_{oc}$  and  $I_{sc}$  values were 6 mV and about 6 nA, respectively. They also used these NFSs to stimulate the fibroblast cells, and found that the L929 cells aligned along the electrospinning direction of the nanofibers. This demonstrated that electrospun P(VDF-TrFE) NFSs have excellent potential for tissue engineering and bone regeneration applications.

## 2.2. Triboelectricity

A triboelectric nanogenerator (TENG) was demonstrated by Wang and co-workers in 2012, and many important advances have been made in this field.<sup>[7,24,32]</sup> The basic mechanism can be briefly described as the combined effect of the conjunction of triboelectrification and electrostatic induction to convert mechanical energy into electricity.<sup>[33]</sup> The triboelectric effect appears between two different materials brought into contact, in which the surfaces of those materials are electrically charged.

In 2014, Zheng et al.<sup>[9]</sup> first demonstrated the feasibility of implanted TENG (iTENG) devices (Figure 2a,b). The primary fabrication materials were Kapton, poly(ethylene terephthalate) (PET), Al film, and poly(dimethylsiloxane) (PDMS). Two different materials were placed facing each other and generated opposite charges when in contact. Then, the surfaces were separated, and a potential difference was generated. The two electrodes attached to the surfaces were connected by a load, and free electrons flowed from one electrode to the other, which generated an opposite potential to balance the induced electrostatic field. Because the cycle of contact and separation occurs during a working period, a PET spacer (400  $\mu\text{m}$ ) was placed between the contact layers. A thin PDMS layer was used as the encapsulation material, owing to its flexibility and biocompatibility. The iTENG was placed under the skin of the left chest, or between the diaphragm and the liver of a live rat, and could harvest the mechanical energy from its periodic breathing. The  $V_{oc}$  and  $I_{sc}$  values were 3.73 and 0.14, respectively. The power density reached up to 8.44  $\text{mW m}^{-2}$ . The converted electricity was stored in a capacitor to drive a prototype pacemaker.

In 2016, Zheng et al.<sup>[8]</sup> achieved the implantation of iTENG devices in large mammals, which were driven by the heartbeat of adult pigs (Figure 2c–e). The *in vivo* output voltage reached up to 14 V, and the corresponding output current increased to 5  $\mu\text{A}$ . In addition, the iTENG was demonstrated to work for over 72 h after implantation, with electricity generated continuously in the active animal. Based on its excellent *in vivo* performance, they fabricated a self-powered wireless transmission system for real-time wireless cardiac monitoring. Furthermore, Zheng et al.<sup>[24]</sup> proposed a biodegradable triboelectric nanogenerator (BD-TENG) to harvest *in vivo* biomechanical energy (Figure 2f–h). They used two different biodegradable materials, poly(lactic-co-glycolic acid) (PLGA) and polycaprolactone (PCL), to fabricate the friction layers, and encapsulated it with PLGA. Therefore, this new type of IVEH can be degraded and resorbed into the subject animal's body. The researchers implanted the device into the subdermal region of the backs of SD rats, and *in vivo* tests demonstrated that the BD-TENG could work for over 24 h with about 3 V output voltage and almost completely dissolved in 72 h.

## 2.3. Automatic Wristwatch

An automatic wristwatch (AW) is a type of self-powered watch using wrist motion as the power source. When the wearer moves, an eccentric oscillating weight in the watch winds a spring, which then turns and spins the pinion. At the same time, a miniature electrical generator driven by the pinion with a few milliseconds generates electrical energy and charges a storage device like a capacitor or rechargeable battery. Researchers utilized this energy transforming mechanism of the automatic wrist watch to harvesting the mechanical energy *in vivo* such as cardiac contraction.

In 1999, Goto et al.<sup>[11]</sup> placed an automatic power-generating system (AGS) based on quartz watch on the right ventricular wall of a dog. The AGS harvested 80 mJ of heart beat energy at about 200  $\text{beats min}^{-1}$  over the course of 30 min, corresponding to about 13  $\mu\text{J}$  per heartbeat.

In 2013, Zurbuchen et al.<sup>[12]</sup> created a mass imbalance oscillation generator (MIOG) by refitting a wrist watch (Figure 3) to harvest the biomechanical energy of a beating heart. The final weight of the modified device was 16.7 g. This energy harvester was sewn onto a sheep's heart using three eyelets of the housing. The results showed that the mean power was 16.7  $\mu\text{W}$ , equal to 11.1  $\mu\text{J}$  energy per heartbeat. A small buffer capacitor was used to store the converted energy, which can power a cardiac pacemaker.

In 2017, Zurbuchen et al.<sup>[10]</sup> fabricated three more MIOGs by removing unnecessary parts to reduce the weight and size. They implanted the MIOGs on different epicardial sites of pigs. The results showed that the output was significantly influenced by the implantation site. These MIOGs can also be connected to buffer capacitors to store the generated energy to power a custom-made cardiac pacemaker.

## 2.4. Biofuel

Biofuel cells, another type of energy harvester with a long history, utilize living organisms to produce electricity. Glucose is a major energy source in living subjects, which can be used as fuel to generate electricity. There are two complementary classes of biofuel cells: microbial and enzymatic fuel cells.<sup>[34,35]</sup> Microbial fuel cells are usually too large to be suitable for *in vivo* applications. Enzyme biofuel cells use enzymes as catalysts to oxidize glucose *in vivo*, and are considered more practical power sources for implantable electronics. In the early enzymatic biofuel cells, the anode and cathode were physical separated to avoid degradation of the enzymes. More recently, researchers have demonstrated using enzyme catalysts on modified electrodes that they can harvest electricity generated by redox reaction between glucose and oxygen in living animals. The redox process can be written as follows



Enzyme-based biofuel cells have been achieved in plants (cacti,<sup>[36]</sup> grapes,<sup>[37]</sup> and oranges<sup>[38]</sup>); mammals (rats<sup>[19,39–41]</sup> and

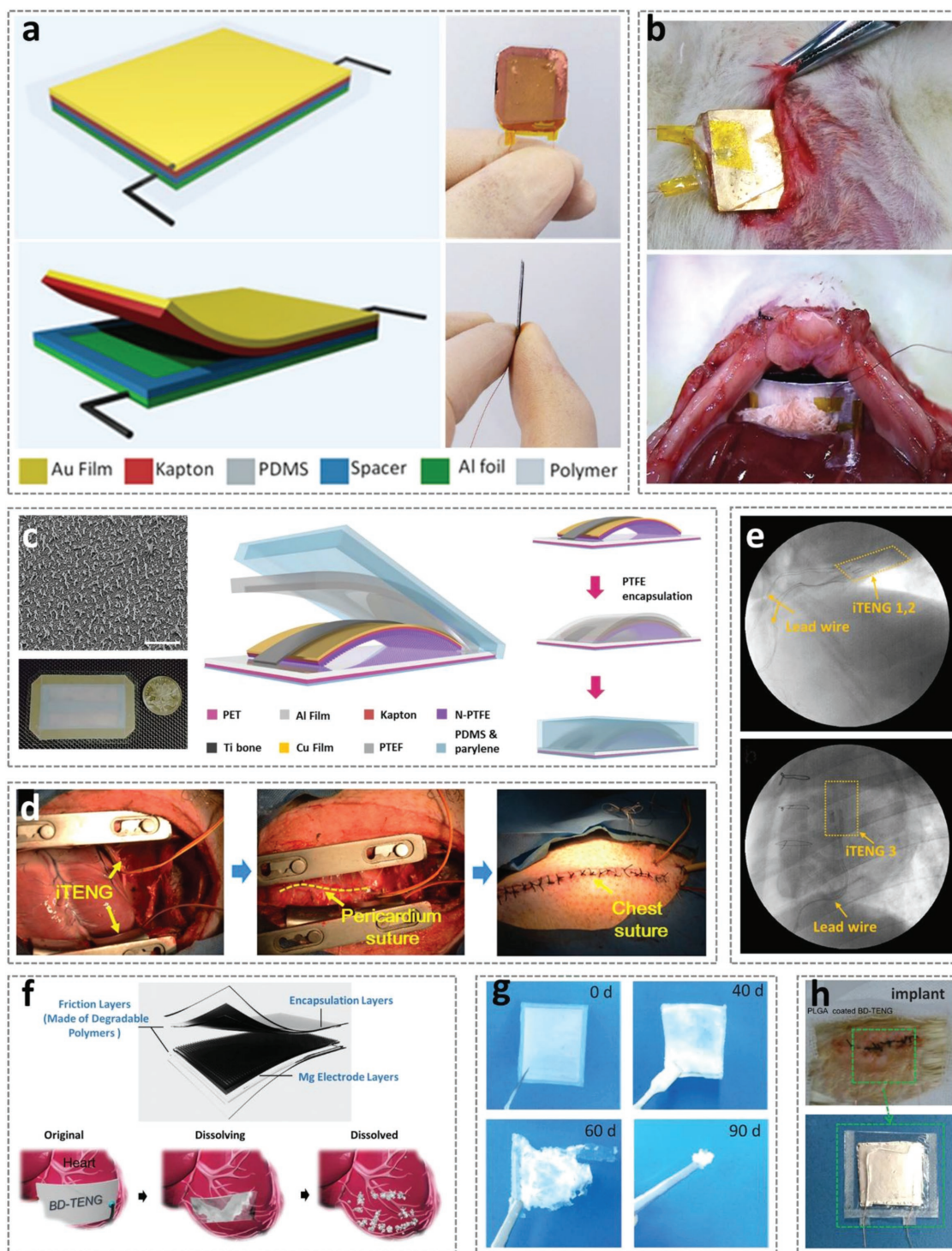


**Figure 2.** a) Schematic diagram and photograph of iTENG for rat. b) iTENG buried under the thoracic skin and attached to a live rat's diaphragm. Reproduced with permission.<sup>[9]</sup> Copyright 2014, Wiley-VCH. c) Schematic diagram and photograph of iTENG for swine. d) iTENGs implanted between the heart and the pericardium of swine. e) Real-time in vivo monitoring of the iTENG by digital radiography imaging. Reproduced with permission.<sup>[8]</sup> Copyright 2016, American Chemical Society. f) Schematic diagram of BD-TENG fixed to pericardium. g) Photographs of BD-TENG at different time periods of the degradation. h) Images of BD-TENG implanted in the subdermal dorsal region of an SD rat. Reproduced with permission.<sup>[24]</sup> Copyright 2016, American Association for the Advancement of Science.

rabbits<sup>[37]</sup>; molluscs (snails<sup>[42]</sup> and clams<sup>[18]</sup>); insects (*Man-duca sexta* (*M. Sexta*),<sup>[43]</sup> and cockroaches<sup>[43–45]</sup>); in lobsters<sup>[17]</sup> (Figures 4 and 5).

In 2010, Flexer and Mano<sup>[36]</sup> proposed using electrodes with immobilized redox enzymes, such as glucose oxidase or bilirubin oxidase, along with redox hydrogels that could harvest

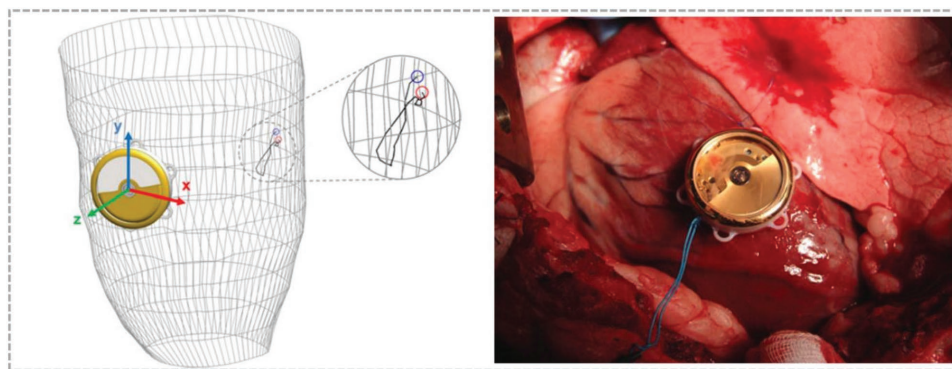


**Figure 3.** Automatic wrist watch based MIOG used for harvesting heart beat energy of sheep. Reproduced with permission.<sup>[12]</sup> Copyright 2012, Springer Nature.

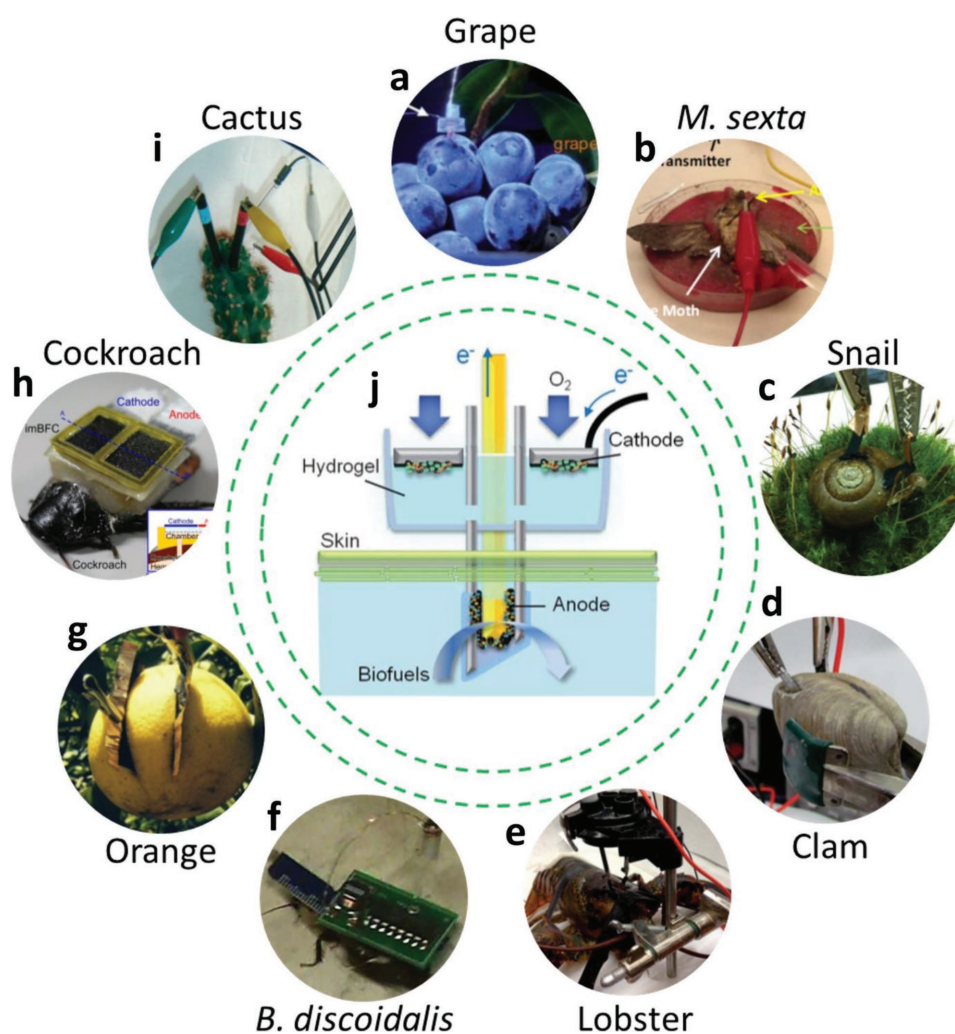


**Figure 4.** Biofuel cells implanted in plants, insects, mollusks, and crustaceans. a) Reproduced with permission.<sup>[37]</sup> Copyright 2011, Royal Society of Chemistry. b) Reproduced with permission.<sup>[43]</sup> Copyright 2015, The Electrochemical Society. c) Reproduced with permission.<sup>[42]</sup> Copyright 2012, American Chemical Society. d) Reproduced with permission.<sup>[18]</sup> Copyright 2012, Royal Society of Chemistry. e) Reproduced with permission.<sup>[17]</sup> Copyright 2012, Royal Society of Chemistry. f) Reproduced with permission.<sup>[43]</sup> g) Reproduced with permission.<sup>[38]</sup> Copyright 2014, Elsevier. h) Reproduced with permission.<sup>[45]</sup> Copyright 2015, Elsevier. i) Reproduced with permission.<sup>[36]</sup> Copyright 2010, American Chemical Society. j) Schematic structure of a biofuel cell. Reproduced with permission.<sup>[37]</sup> Copyright 2011, Royal Society of Chemistry.

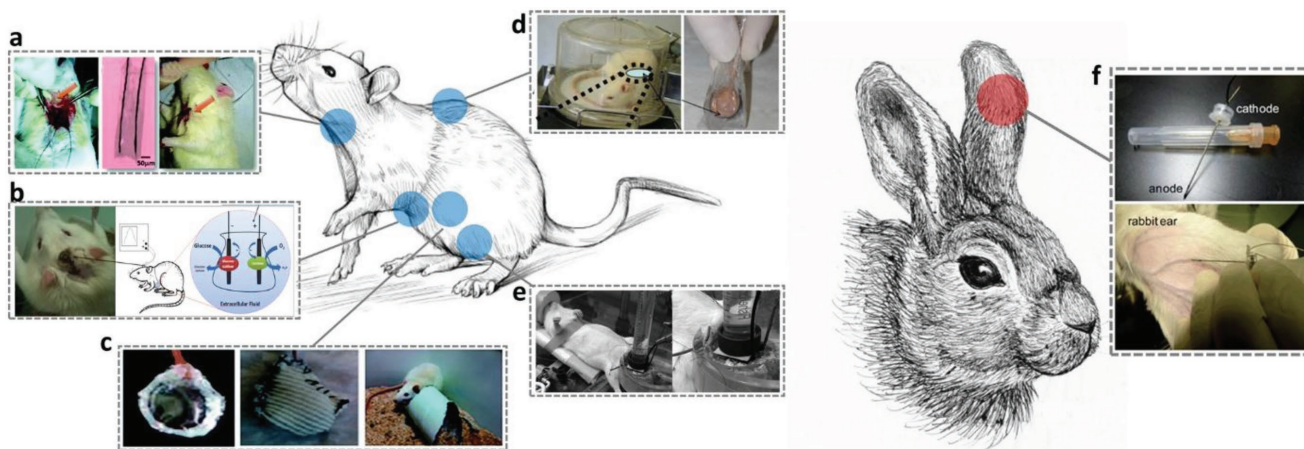


**Figure 5.** Biofuel cells implanted in mammals. a) Implanting site: Jugular vein of rat. Year: 2013. Reproduced with permission.<sup>[46]</sup> Copyright 2012, Royal Society of Chemistry. b) Implanting site: Retroperitoneal space in left lateral position of rat. Year: 2013. Reproduced with permission.<sup>[19]</sup> Copyright 2013, Springer Nature. c) Implanting site: Retroperitoneal space in the left lateral position. Year: 2015. Reproduced with permission.<sup>[40]</sup> Copyright 2015, Royal Society of Chemistry. d) Implanting site: Retroperitoneal space in left lateral position of rat. Year: 2010. Reproduced with permission.<sup>[39]</sup> Copyright 2010, PLOS. e) Implanting site: Rat cremaster tissue. Year: 2013. Reproduced with permission.<sup>[41]</sup> Copyright 2013, Wiley-VCH. f) Implanting site: Blood vessel in a rabbit ear. Year: 2011. Reproduced with permission.<sup>[37]</sup> Copyright 2011, Royal Society of Chemistry.

energy from the glucose and  $O_2$  produced during photosynthesis. These electrodes were implanted into a living cactus leaf and responded dynamically to visible light in real time. Cinquin et al.<sup>[39]</sup> presented functional *in vivo* glucose biofuel cells, which were implanted into the retroperitoneal space of freely moving rats (Figure 5b). Specifically, their cells used based on polyphenol oxidase (PPO)/quinone at the cathode, and composite graphite discs containing glucose oxidase/ubiquinone at the anode. The electrodes were modified with enzymes that were not covalently bound to the surface of the electron collectors, but instead made use of an innovative and simple mechanical confinement of process involving various enzymes and redox mediators.

In 2011, Miyake et al.<sup>[37]</sup> fabricated bioanodes, including a needle for accessing the biofuels in living organisms through the skin, and a gas-diffusion alternative for utilizing the oxygen in the air. They implanted a bioanode in a raw grape, and obtained a maximum power of  $26.5 \mu\text{W}$  at  $0.34 \text{ V}$ . Then, they inserted a needle anode into a blood vessel in a rabbit's ear to investigate power generation from blood sugar (Figure 5f). The power from this cell was  $0.42 \mu\text{W}$  at  $0.56 \text{ V}$ . In addition to energy harvesting, these bioanodes could act as self-powered glucose monitors in the organisms.

In 2012, Rasmussen et al.<sup>[44]</sup> used enzymatic electrodes to convert trehalose from insects and oxygen from the air into electricity. They implanted electrodes into the abdomen of a female *Blaberus discoidalis* (*B. discoidalis*) through two incisions. The maximum power density was about  $55 \mu\text{W cm}^{-2}$  at  $0.2 \text{ V}$ , but decreased by  $\approx 5\%$  after about 2.5 h of *in vivo* operation. The Katz' and co-workers reported an implanted biofuel cell operating in snails<sup>[42]</sup> and clams.<sup>[18]</sup> The biocatalytic electrodes were based on nanostructured "buckypaper" composed of compressed multiwalled carbon nanotubes modified with oxygen-insensitive pyrroloquinoline, quinone-dependent glucose dehydrogenase, and oxygen-reducing laccase. A biofuel cell implanted in a snail remained operational for several months. The researchers placed biocatalytic electrodes in clams and

studied the output when three clams were connected in parallel or in series. They found values of  $V_{oc} \approx 360 \text{ mV}$  and  $I_{sc} \approx 300 \mu\text{A}$  ( $\approx 1.2 \text{ mA cm}^{-2}$ ) for the parallel configuration, and  $V_{oc} \approx 800 \text{ mV}$  and  $I_{sc} \approx 25 \mu\text{A}$  ( $\approx 100 \mu\text{A cm}^{-2}$ ) for the serial circuitry. Yoshino et al.<sup>[20]</sup> presented a bioelectrocatalytic architecture using PVI-[Os(bby)<sub>2</sub>Cl] and glucose oxidase (GOD) inside an aligned carbon nanotube forest (CNTF) film. The device was inserted into a grape and used to power light-emitting diode (LED).

In 2013, MacVittie et al.<sup>[17]</sup> implanted enzyme-based biofuel cells into living lobsters. The typical outputs from one lobster were  $V_{oc} \approx 0.54 \text{ V}$  and  $I_{sc} \approx 1 \text{ mA}$ . To enhance the output voltage, the researchers connected two "electrified" lobsters in series, and used them to directly power an electric watch. In the same year, Sales et al.<sup>[46]</sup> investigated an implantable glucose/dioxygen enzyme and Pt hybrid micro-biofuel cell, which was placed into the jugular vein of a living rat (Figure 5a). Zebda et al.<sup>[19]</sup> described an implanted glucose biofuel cell (GBFC) that was able to extract energy from mammalian body fluids. Furthermore, they performed a long-term implantation experiment lasting for 110 d (Figure 5b). Castorena-Gonzalez et al.<sup>[41]</sup> assembled enzyme modified electrodes in human serum solutions and placed them onto exposed rat cremaster tissue. The *in vivo* tests showed that the  $V_{oc}$  and  $I_{sc}$  values were  $140 \pm 30 \text{ mV}$  and  $10 \mu\text{A}$ , respectively (Figure 5e).

In 2014, Schwefel et al.<sup>[43]</sup> implanted trehalose/oxygen biofuel cells into cockroaches (*B. discoidalis*) and moths (*M. sexta*), which were used to power custom-designed oscillators mounted on the backs of the insects for wireless communication. In the case of live moths, the biofuel cell can generate an areal power density of  $15.6 \mu\text{W cm}^{-2}$ . This demonstrated the potential that biofuel cells possess to construct self-powered "cyborg" insects.

In 2015, El Ichi et al.<sup>[40]</sup> used a 3D-nanofibrous network of compressed chitosan containing genipin, carbon nanotubes, and laccase to fabricate a new GBFC (Figure 5c). To reduce the effects of the extracellular fluids at physiological pH on the function of the GBFC function, they demonstrated the encapsulation of laccase in a composite of Chit-MWCNT (compressed

laccase – carbon nanotube) fibers. They implanted the biocathodes in rats and a long-term *in vivo* test over 167 d was performed to study the biocompatibility and biodegradability of the encapsulated device. MacVittie et al.<sup>[38]</sup> implanted catalytic electrodes into orange pulp. The open-circuit voltage, short-circuit current density, and maximum power produced by the GBFC, were  $\approx 0.6$  V,  $\approx 0.33$  mA cm<sup>-2</sup>, and 670  $\mu$ W, respectively.

In 2016, Shoji et al.<sup>[45]</sup> investigated an insect-mountable enzymatic biofuel cell (im-BFC) that generated electricity from trehalose in insect hemolymph, by mounting them onto cockroaches. The imBFC has the potential to act as a power supply for insect cyborgs, *in vivo* microrobots, as well as for other systems. Researchers also demonstrated, in 2017, an energy-harvesting galvanic cell placed in the gastrointestinal tract, which can be used for powering *in vivo* temperature sensors and wireless communication devices.<sup>[47]</sup>

## 2.5. Endocochlear Potential

Endocochlear potential (EP) is an electrochemical gradient in the cochlear endolymphatic spaces, which is the main driving force for the cochlear mechanotransduction of sound pressure

vibrations into neurotransmitter signals at the auditory nerve. Mercier et al.<sup>[21]</sup> demonstrated an *in vivo* power source based on the endocochlear potential generated by K<sup>+</sup> ion transfer between the perilymphatic and endolymph (Figure 6). The voltage and current were 70–100 mV and 14–28  $\mu$ A, respectively. They fabricated a microelectronic chip of size of  $2.4 \times 2.4 \times 0.2$  mm<sup>3</sup> enabled wireless radio transmission. They inserted two electrode tips into the cochlea, and the electrode shafts were connected to a microelectronic chip located outside of a guinea pig. They operated the chip using the EP of an anesthetized guinea pig as the energy source for up to 5 h, which is equivalent to the power of a 2.4 GHz radio transmitting monitoring signals from the EP every 40–360 s.

## 2.6. Optical Energy

Solar energy is an abundant and clean power source in the ambient environment, and solar cells possess a long history. Researchers have utilized solar cells to power IMEs, and have implanted them in rats, rabbits, and pigs.

In 2004, Laube et al.<sup>[13]</sup> confirmed the feasibility of using a photovoltaic device as part of an intraocular lens (IOL) in an epiretinal implant with long-term functionality in rabbits, which

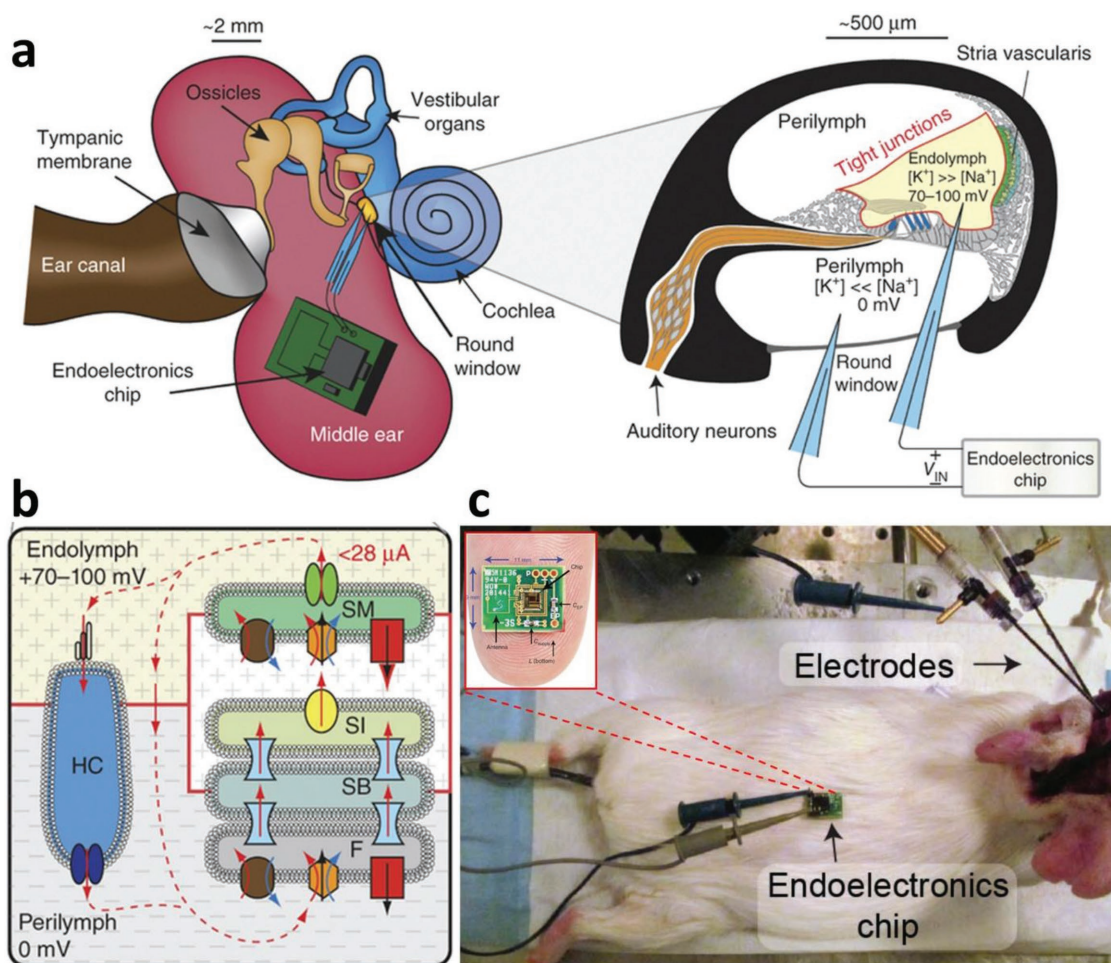


**Figure 6.** a) Schematic of the EP type of IVEH. b) Schematic of the equivalent circuit model of the endocochlear potential. c) Photograph of the prototype endoelectronics board on a human index finger and the implanted experiment. Reproduced with permission.<sup>[21]</sup> Copyright 2012, Springer Nature.

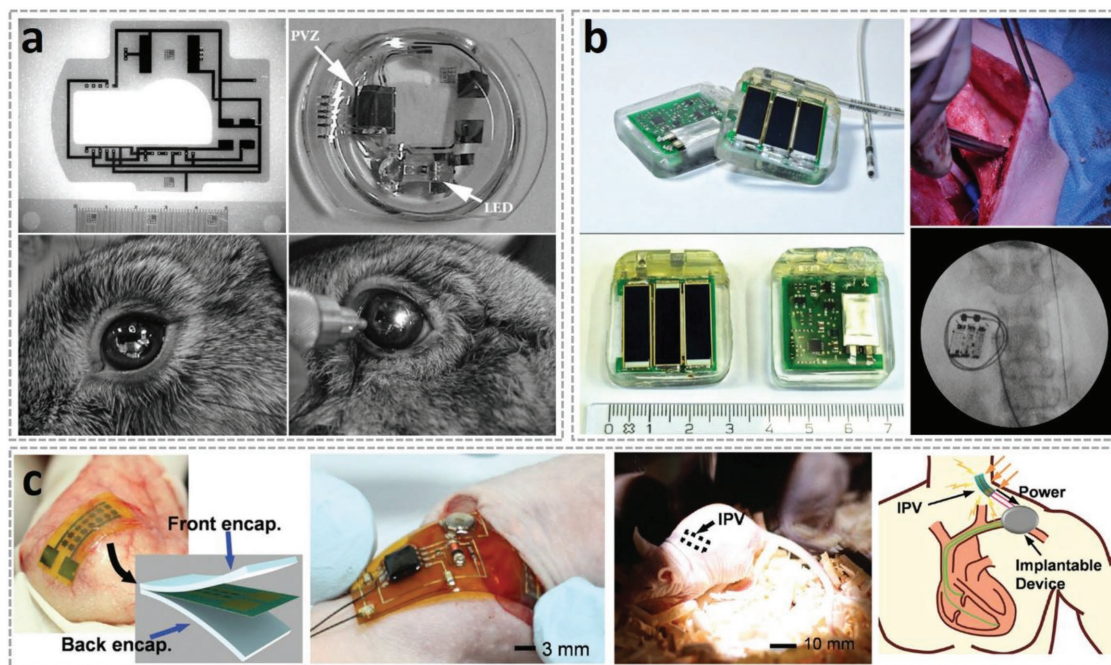


**Figure 7.** a) Photovoltaic cells based IOL were implanted in the capsular bag after phacoemulsification in rabbit. Reproduced with permission.<sup>[13]</sup> Copyright 2004, Springer Nature. b) The sunlight-driven pacemaker prototype was subcutaneously implanted in pig. Reproduced with permission.<sup>[14]</sup> Copyright 2015, Elsevier. c) The implanted photovoltaic (IPV) and self-powered cardiac pacemaker were implanted into a live hairless mouse. Reproduced with permission.<sup>[15]</sup> Copyright 2016, Wiley-VCH.

can transfer optical energy to power an intraocular microsystem (Figure 7a). IOLs consist of photovoltaic cells (PVC) and a LED. The primary material used to fabricate the PVC was gallium arsenide (GaAs). The dimensions were 1.7 mm × 2 mm. Two or three PVC connected in series generated  $V_{oc}$  values of 2 V or 3 V, respectively. The optical-to-electrical power conversion efficiency reached 40%. The LED served as a signal to show if that the energy transmission was successful. The light source was an 850 nm infrared laser beam. The researchers completed a long-term test in rabbits, which demonstrated that the longevity of the microsystems ranged from 14 d to over 7 months.

In 2014, Haeberlin et al.<sup>[148]</sup> used three commercial solar cells, connected in series and placed under pig skin flaps, to convert sunlight into electricity. The total effective area was 3.24 cm<sup>2</sup>. The  $V_{oc}$  of the entire solar module reached 5.67 V. The output was closely related with the implantation depth. Their measurements *in vivo* yielded a median output power density of >3500  $\mu\text{W cm}^{-2}$  when the skin flap thickness was 2.8–3.84 mm. They successfully powered a pacemaker with this implanted solar cell.

In 2015, Haeberlin et al.<sup>[14]</sup> developed a battery-less pacemaker powered by solar modules consisting of three monocrystalline solar cells connected in series (Figure 7b). This pacemaker was implanted subcutaneously into a pocket in the right lateral neck of a pig.

In 2016, Song et al.<sup>[15]</sup> described IVEHs based on ultrathin photovoltaics, and integrated them with a rechargeable battery and a custom-built pacemaker on a flexible substrate (Figure 7c). The entire system was implanted into a live hairless mouse to harvest optical energy through the skin. The energy generated was stored in the battery, which, in turn powered the pacemaker.

### 3. Comparisons

#### 3.1. Fabrication

The manufacturing process for IVEHs primarily includes micro/nanofabrication steps, along with material synthesis and preparation technologies. The materials, structures, and complexity largely determine the overall cost of an IVEH, which is an important factor for commercialization, as shown in Table 1.

The structures of piezoelectric and triboelectric devices include layers, nanowires, or fibers. The cost of piezoelectric devices is usually high because of the complex and sophisticated micromachining technologies required. For instance, a PZT-based multilayered mechanical energy harvester can be made using methods such as electron beam evaporation, photolithography, reactive ion etching, or transfer-printing.<sup>[5,6]</sup> Triboelectric IVEHs have some significant advantages, such as low cost, robustness, and environmental friendliness owing to the natural abundance of the starting materials, flexible structures, and ease of manufacturing. The triboelectric effect appears between any two materials with different triboelectricities, such as metal and a polymer, during a contact and separation cycle. Thus, a range of material groups can be used to fabricate IVEHs that are low-cost, flexible, reliable, biocompatible, and exhibit high outputs.

The conversion of energy using biofuel cells is a chemical process, therefore, the manufacturing considerations are different than those with the fabrication of piezoelectric or triboelectric devices. Most significantly, the structures and processing methods associated with biofuel cells are simpler than with the physical energy conversion devices.

**Table 1.** The comparison of fabrication related to IVEHs.

Types	Materials	Structures	Manufacturing technologies	Animal experiments	Cost
	PZT	Multilayers	photolithography/wet chemical etching/reactive ion etching/electron beam evaporation/sputtering/aerosol deposition/laser lift-off/spincoating/hard baking/electric field poling/transfer printing	bovine/sheep/pig	high
Piezo-device	ZnO	Single nanowire	Physical vapor deposition	Rat	High
	PVDF	Thin film/nanofibers	Acid etching/electrospinning/electric field poling	Rat/pig	High
TENG	Two materials with different tribo polarities	Double contacting layers	Spin-coating/hard baking	Rat/pig	Low
AW	Refitted commercial automatic wristwatch	Bulk	–	Dog/sheep	Low
Biofuel	Enzyme/metal electrode	Needles	Soft lithography/electrodeposition/screen-printing	Rat/rabbit/lobster/mollusc/insect/plant	Low
EP	Glass microelectrodes	Double tips	Microfabrication technologies	Rat	High
Optical energy	Solar cells	Bulk/thin film	Wet chemical etching/sputtering/electron beam evaporation	Rabbit/pig/rat	High

Hybrid methods are also commonly used to fabricate IVEHs. For example, ZnO nanoparticles are mixed with a PVDF solution to fabricate thin-film IVEHs.<sup>[28]</sup> The hybrid enzyme/Pt micro-biofuel cell was demonstrated to be able to extract energy from the jugular vein of a living rat.<sup>[46]</sup> In addition to the design of the structure, researchers optimize the hybrid energy harvesting devices. The hybrid energy harvesters based on the various field couplings include piezoelectric-triboelectric,<sup>[49,50]</sup> piezoelectric-electromagnetic,<sup>[51]</sup> piezoelectric-photovoltaic,<sup>[52]</sup> piezoelectric-pyroelectric,<sup>[53]</sup> piezoelectric-pyroelectric-photovoltaic,<sup>[54]</sup> piezoelectric-biofuel,<sup>[55]</sup> triboelectric-electromagnetic,<sup>[56]</sup> triboelectric-electrochemical,<sup>[57]</sup> triboelectric-photovoltaic,<sup>[58]</sup> triboelectric-pyroelectric-photovoltaic,<sup>[59]</sup> triboelectric-pyroelectric-piezoelectric,<sup>[60]</sup> and photovoltaic-pyroelectric.<sup>[61]</sup> In addition, material or structural hybrids, for example, Kevlar microfiber-ZnO nanowires,<sup>[62]</sup> (BaTi(1-x)ZrxO<sub>3</sub>)-PVDF,<sup>[63]</sup> ZnO nanowire-PVDF,<sup>[64]</sup> BaTiO<sub>3</sub> nanowire-PVC fibers,<sup>[65]</sup> ZnSnO<sub>3</sub>-MWCNTs,<sup>[66]</sup> ZnSnO<sub>3</sub> nanocube-polymers,<sup>[67]</sup> grapheme oxide-ZnO,<sup>[68]</sup> carbon fiber-ZnO nanowire-paper,<sup>[69]</sup> and MPP-ZnO<sup>[70]</sup> have also been used. These hybrid energy harvesting methods are instructive references for IVEHs, but there are significant differences between these new concepts and devices that have actually been implanted.

### 3.2. Energy Output

Energy Output is a key factor for IVEHs. To our knowledge, IMEs, such as cardiac pacemakers and deep brain stimulators, generally require 2–3 V operation. However, most recent IVEHs, especially biofuel cells (≈0.5 V), are not up to this standard. The output properties of IVEHs are shown in **Figure 8**.

To increase the outputs, researchers have put forward various methods, including the connection of multiple devices, or storing generated energy in buffers such as capacitors or rechargeable batteries.<sup>[17]</sup> For instance, three clam biofuel cells were connected in parallel and in series, respectively. The

harvested energy was stored in a capacitor to power an electrical motor.<sup>[18]</sup> This approach has also been used for biofuel cells in living lobsters.<sup>[17]</sup> Researchers connected two lobster-biofuel cells in series to increase the output voltage from 0.6 to 1.2 V, which was able to power an electric watch for over one hour. It was worth mentioning that, if implanting two pairs of electrodes into the same lobster, the output did not increase linearly, and was less than double the voltage of a single electrode pair. The results could be explained by the equivalent resistance of the lobster's body tissue, resulting in a low impedance path between the anodes and cathodes, which prevented the desired series operation of the two fuel cells.

Connection of multiple devices is also commonly done in piezoelectric,<sup>[5,6,71]</sup> triboelectric,<sup>[9]</sup> and optical<sup>[15]</sup> IVEHs. For example, connections have been made both in parallel and in series configurations in multilayer IVEH based on PZT ribbons to increase the output voltage.<sup>[5]</sup> Researchers fabricated an IVEH array using the parallel connection of four iTENGs, and found that the short-circuit current increased fourfold compared with that of a single iTENG. Also, 14 microsolar cells were connected in parallel or in series, which enhanced the value of  $I_{sc}$  about sevenfold, and approximately doubled  $V_{oc}$ .<sup>[15]</sup>

In addition, the output properties of IVEHs are related to the load impedance. For example, the internal resistance of biofuel cell is about 200 Ω–20 kΩ.<sup>[17,18,38,41,42]</sup> Compared with the low internal resistance of biofuel cells, the corresponding values for TENG are high, around 20–80 MΩ.<sup>[9,24]</sup> In general, high internal resistance causes a voltage drop, which results in lower output capability. For most mechanical-to-electrical energy transduction IVEHs, the outputs are usually AC, and some of them give high output voltage but low current, so are not directly applicable to active implantable electronic medical devices. Therefore, the application of power management is important for IVEHs. A common way to convert from AC to DC current is by including a rectifier, but this results in a decrease in power for the IVEH. The outputs of the mechanical-to-electrical IVEHs are also distinctly affected by the external driving forces. For

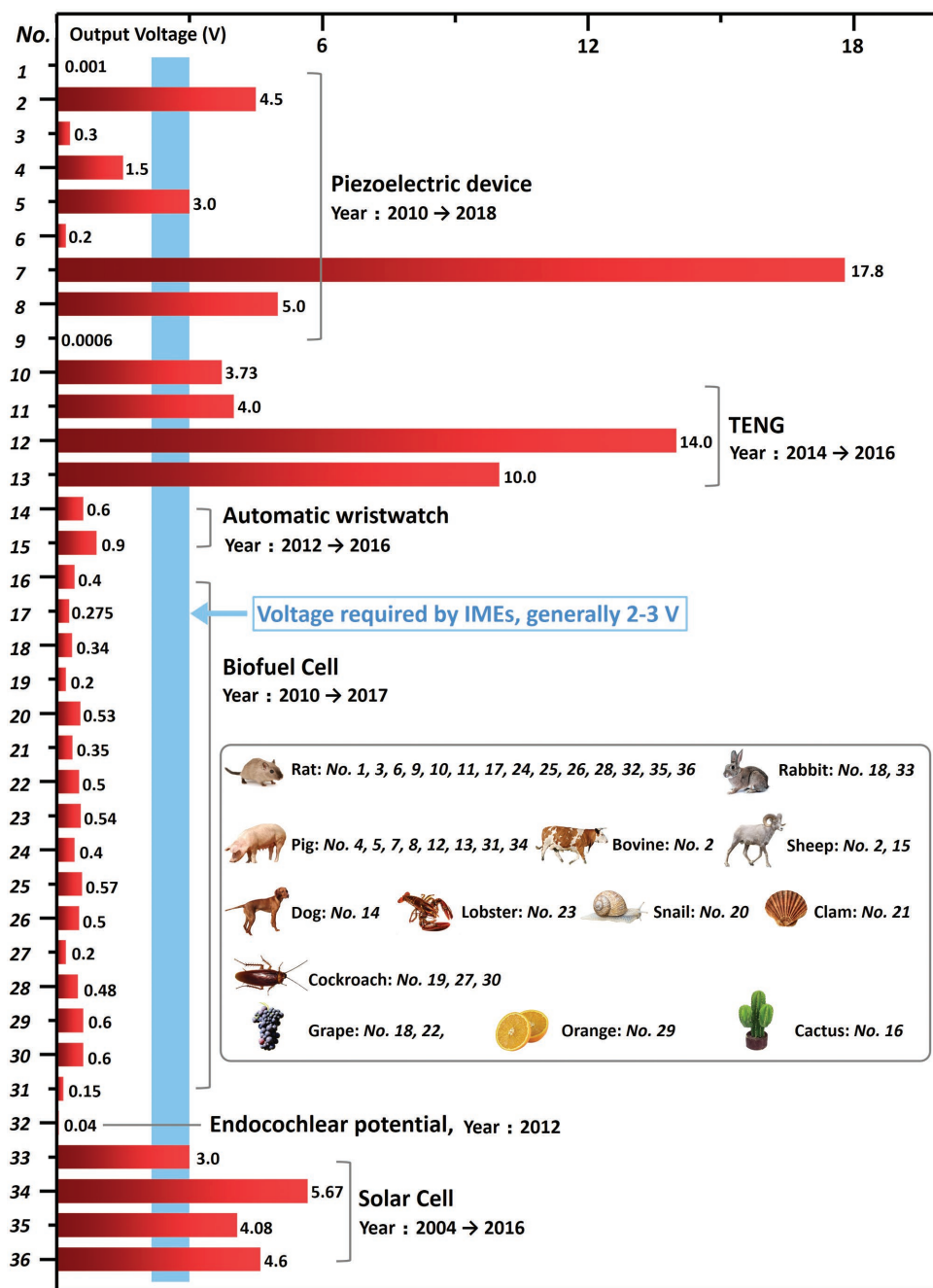


**Figure 8.** The output voltage of IVEHs. Ref: No. 1-Li et al., 2010.<sup>[4]</sup> 2-Dagdeviren et al., 2014.<sup>[5]</sup> 3-Yuan et al., 2014.<sup>[74]</sup> 4-Zhang et al., 2015.<sup>[26]</sup> 5-Lu et al., 2015.<sup>[6]</sup> 6-Yu et al., 2016.<sup>[28]</sup> 7-Kim et al., 2017.<sup>[30]</sup> 8-Jeong et al., 2017.<sup>[29]</sup> 9-Wang et al., 2018.<sup>[31]</sup> 10-Zheng et al., 2014.<sup>[9]</sup> 11-Zheng et al., 2016.<sup>[24]</sup> 12-Zheng et al., 2016.<sup>[8]</sup> 13-Ma et al., 2016.<sup>[22]</sup> 14-Goto et al., 1999.<sup>[11]</sup> 15-Zurbuchen et al., 2013.<sup>[12]</sup> 16-Flexer et al., 2010.<sup>[36]</sup> 17-Cinquin et al., 2010.<sup>[39]</sup> 18-Miyake et al., 2011.<sup>[37]</sup> 19-Rasmussen et al., 2012.<sup>[44]</sup> 20-Halamkova et al., 2012.<sup>[42]</sup> 21-Szczupak, et al., 2012.<sup>[18]</sup> 22-Yoshino et al., 2013.<sup>[20]</sup> 23-MacVittie et al., 2013.<sup>[17]</sup> 24-Sales et al., 2013.<sup>[46]</sup> 25-Zebda et al., 2013.<sup>[19]</sup> 26-Castorena-Gonzalez et al., 2013.<sup>[41]</sup> 27-Schwefel et al., 2014.<sup>[43]</sup> 28-El Ichi et al., 2015.<sup>[40]</sup> 29-MacVittie et al., 2015.<sup>[38]</sup> 30-Shoji et al., 2016.<sup>[45]</sup> 31-Nadeau et al., 2017.<sup>[47]</sup> 32-Mercier et al., 2012.<sup>[21]</sup> 33-Laube et al., 2004.<sup>[13]</sup> 34-Haerberlin et al., 2014.<sup>[48]</sup> 35-Haerberlin et al., 2015.<sup>[14]</sup> 36-Song et al., 2016.<sup>[15]</sup>

example, the in vitro and in vivo studies of a piezoelectric generator (PG) by Zhang et al. showed that the output was related with the tightness of wrapping around the ascending aorta. By restricting the deformation of the PVDF film, the output of the device was impaired.<sup>[26]</sup> Therefore, managing the electrical

output of IVEHs is an important step for improved the utilization of the harvested energy.

The outputs and energy conversion efficiency characteristics of intraharvesting of IVEHs depend on energy forms and related converting methods, equivalent circuits of the whole

energy harvesting systems, and internal environment in the organism. For instance, compared to biofuel cells, IVEHs based on piezoelectric and triboelectric devices convert energy by physical means, which have higher output voltage but lower current *in vivo*. Therefore, a full range of multiangle consideration should be required during design and fabrication of IVEHs with significant performance.

### 3.3. Encapsulation

The internal environment of organisms is a place filled with chemical, mechanical, electrical, and saline reactions, in which the available space for implanted devices is limited.<sup>[72]</sup> For most IVEHs, encapsulation is essential for preventing damage to the devices due to body fluids and tissue. The encapsulation materials must be biocompatible, flexible, and stable, which can minimize the risks of leakage and immune responses.<sup>[5,73]</sup>

At present, the most commonly used materials are PI,<sup>[5,26]</sup> silicone, PDMS,<sup>[4,9,13,15,19,40,48]</sup> poly(tetrafluoroethylene) (PTFE),<sup>[39]</sup> dialysis membranes,<sup>[19]</sup> chitosan,<sup>[40]</sup> and Dacron bags.<sup>[19,40]</sup> The structures of encapsulation can be divided into two classes—those with a single layer of only one type of material, and those multilayered with several materials.<sup>[19,40]</sup> Although multiple process can improve encapsulation performance, the mechanical properties may be significantly changed, resulting in negative effects after implantation, particularly damage to organs and tissues. However, encapsulation will also affect the output performance of the IVEH. For example, piezoelectric and triboelectric devices harvest energy by converting mechanical motion into electricity. Inevitably, encapsulation will change the mechanical properties of these devices, including ZnO nanowires, PZT films, and TENG, which may make deformation more difficult under the applied external force.

Meanwhile, for some IVEHs with spacer structures, inappropriate packaging can impair the power generation process. For example, in TENG devices, spacer structures ensure that the contact and separation processes occur during operation. Researchers have developed a polymer frame and “keel structure,” consisting of a highly resilient titanium strip, to act as spacer.<sup>[8,22]</sup>

Researchers have found that encapsulation with silicone alone was not enough to seal the implant completely for use in a rabbit’s eye.<sup>[13]</sup> Therefore, they added parylene C, which has negligible permeability, excellent adhesive strength to silicone, and good *in vivo* biocompatibility to improve the hermetic sealing. Also, other researchers have used inorganic materials, such as Al<sub>2</sub>O<sub>3</sub> deposited on the organic encapsulation material, to fill the gaps between the polymer chains. This could enhance the water-resistance and anti-corrosion performance of the encapsulation layer.<sup>[73]</sup>

Conversely, biofuel cells should not be encapsulated in order to keep the two modified bioelectrodes in contact with the body fluids. However, this open structure has shortcomings, including the risk of external leakage of the bioelectrode components and enzymes from the electrodes into the body.<sup>[19]</sup>

The quality of encapsulation directly affects the *in vivo* function and property of IVEHs. The main considerations for the improvement of encapsulation are related to synthesis and preparation of new material, fully sealed methods, ultraflexible structures, biocompatibility, and long-term effectiveness. The encapsulation technology of IVEHs still has extensive upgrade space.

### 3.4. Durability Testing

As of now, only some IVEHs have passed long-term *in vivo* tests. The longest was seven months in rabbit,<sup>[13]</sup> and the shortest was 5 h in a rat<sup>[21]</sup> (Figure 9). Remarkably, biofuel cell IVEHs survived 110 d of testing when encapsulated in a Dacron bag. The purpose of encapsulation was to prevent external leakage of the bioelectrode components from the device, and to preserve the activity of the enzymes at the bioelectrodes from being inhibited by the body fluids or biological macromolecules. This closed structure was more stable than the open structure consisting of two bare electrodes. In addition, researchers have shown that IVEHs based on PZT or TENG can operate normally in awake or ambulating swine for 48 and 72 h, respectively.<sup>[8,71]</sup>

It can be seen from these comparisons that biofuel cell IVEHs can be implanted *in vivo* with long functional lifetimes,

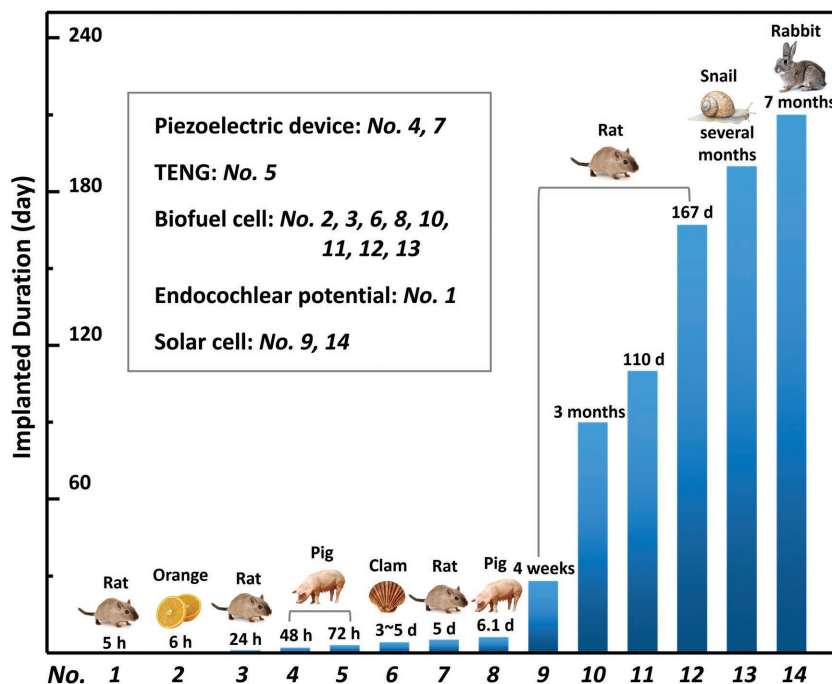


**Figure 9.** The implanted duration of IVEHs so far. Mercier et al.<sup>[21]</sup> MacVittie et al.<sup>[38]</sup> Sales et al.<sup>[46]</sup> Dagdeviren et al.<sup>[71]</sup> Zheng et al.<sup>[8]</sup> Szczupak et al.<sup>[18]</sup> Yu et al.<sup>[28]</sup> Nadeau et al.<sup>[47]</sup> Song et al.<sup>[15]</sup> Cinquin et al.<sup>[39]</sup> Zebda et al.<sup>[19]</sup> El Ichi et al.<sup>[40]</sup> Halamkova et al.<sup>[42]</sup> Laube et al.<sup>[13]</sup>

largely because the structures of biofuel cell IVEHs are simpler, and that the fuel used for energy conversion is continuously available. For an optimistic scenario in which IVEHs are routinely used in the human body to become reality, additional lifetime testing, especially in large mammals, must be done. This requires solving three key problems: 1) Increasing the output of IVEHs, 2) finding appropriate implantation sites, and 3) reducing the side effects on the organs when designing devices impervious to in vivo environments.

## 4. Challenges and Perspectives

### 4.1. Miniaturization

With the remarkable improvements in material science and engineering, along with those in micro and nanofabrication techniques, IMEs can be made smaller and more highly integrated. For most IMEs, the batteries or other power sources primarily determine the weight and size, which is one of the biggest obstacles to the miniaturization of IMEs.<sup>[75]</sup> Therefore, finding ways to minimize the weight and size, while still ensuring sufficient energy capacities for these power supplies, is crucial for implantable electronics. IVEHs that harvest energy from the surrounding environment enable the production of IMEs that are less dependent on large-capacity batteries, and allow for significant miniaturization.

For early biofuel cell IVEHs, the physical separation of the anode and cathode owing to cell membrane necessitated large devices. To resolve this problem, researchers demonstrated a structured biofuel cell without a membrane by immobilizing enzymes on electrodes or using direct electron transfer between the redox enzyme and the electrodes.<sup>[35]</sup>

Miniaturization is not just a matter of reducing the physical size of IVEHs, since the resulting changes in fluid dynamics, effects on implantation sites, increased internal resistances, and reductions in power output must also be considered, which often require completely different design strategies. For most, the output performances are positively correlated with the size of the devices. That is, a smaller size means lower outputs. Therefore, maintaining as high an output level as possible is a challenging issue for miniaturization of IVEHs. The feasible solutions to miniaturization of IVEHs should be based on fabricating devices with higher outputs and energy conversion efficiency, ultrathin and flexible encapsulation materials and structures, and flexible integrated circuit technology. With the development of material science, electronic engineering and micromachining techniques, those smaller, longer-lasting, and more functional implantable IVEHs are becoming possible.

### 4.2. Connection

Connections are important for IVEHs, IMEs, and other implanted electronics. Electrical wires, such as those made from gold,<sup>[43]</sup> copper,<sup>[30,39,40,47]</sup> PTFE,<sup>[71]</sup> carbon paste,<sup>[19]</sup> or sputtered metals, like Au or Pt<sup>[5,6,15]</sup> are commonly used. An important use is to connect multiple modules in an IVEH to

improve the output properties. Song et al.<sup>[15]</sup> used sputtered Ti or Au to connect 14 solar microcells, which enhanced the  $V_{oc}$  from 2.3 to 4.6 V, and the  $I_{sc}$  from 57 to 400  $\mu$ A. Some typical connection methods in IVEHs are shown in **Figure 10**.

Another purpose of connection is to link IVEHs with external electronics. PZT energy harvesters can be connected to monitors using flexible ACF (anisotropic conductive film) cables to enable that the correct output voltage is measured<sup>[6]</sup> (Figure 10b). In addition, these ACF cables can be used to connect the IVEH to rectifier and microbattery to form integrated self-powered energy system<sup>[5]</sup> (Figure 10d).

The connectors used in IVEHs should have long-term geometric and mechanical stability, as well as reliable signals and steady power transmission. With the development of complicated functional implantable devices, the connectors become more and intricate. Shi et al.<sup>[50]</sup> demonstrated a new type of connector for IVEHs and implantable electronics, which combined of advantages of conventional connectors, which allowed for both power generation as well as signal transmission. This connector was composed of three main components: a plug, a socket, and a cavity. Since some IVEHs need to be located at narrow and soft position, these connectors have been used to provide design flexibility, and can even be fabricated from flexible materials, such as like conducting polymers (Figure 10e).

Connections between IVEHs and commercial implantable electronics are directly related to the success of self-powered implantable electric systems. For example, the most used commercial cardiac pacemaker is generally implanted under the skin near clavicle, but the reported IVEHs converting heart beat mechanical energy were placed on the surface of heart.<sup>[4,5,22,30]</sup> Therefore, the way to connect both is crucial to form a self-powered cardiac pacemaker which can be used in clinic. The method of connections has been one of the most desirable research aspects in the self-powered IMEs.

### 4.3. Power Management

Effective power management greatly enhances the efficiency of the energy harvested by IVEHs. In general, there are two basic modes for energy usage, along with and corresponding design strategies for power management (**Figure 11**):

- 1) Storing the generated energy: The output of some IVEHs come in periodic pulses. For example, piezoelectric and triboelectric IVEHs can be implanted at certain sites near moving organs, such as the pericardial sac, heart, lungs, or diaphragm, and are driven by the motions of those organs. Pulsed outputs are synchronized with the cardiac beats or respiratory rate, so they are not able to power IMEs directly. Hence, energy-storage devices, like rechargeable batteries or capacitors, are required here. In addition, because these devices generally have high impedances (around 8–10 M $\Omega$ ),<sup>[8,24]</sup> the problem of impedance mismatch may induce significant energy losses when the generated energy is sent into a battery. Researchers demonstrated some methods to alleviate this issue. Niu et al.<sup>[76]</sup> presented a two-stage power management circuit for TENG. At the first stage, the energy

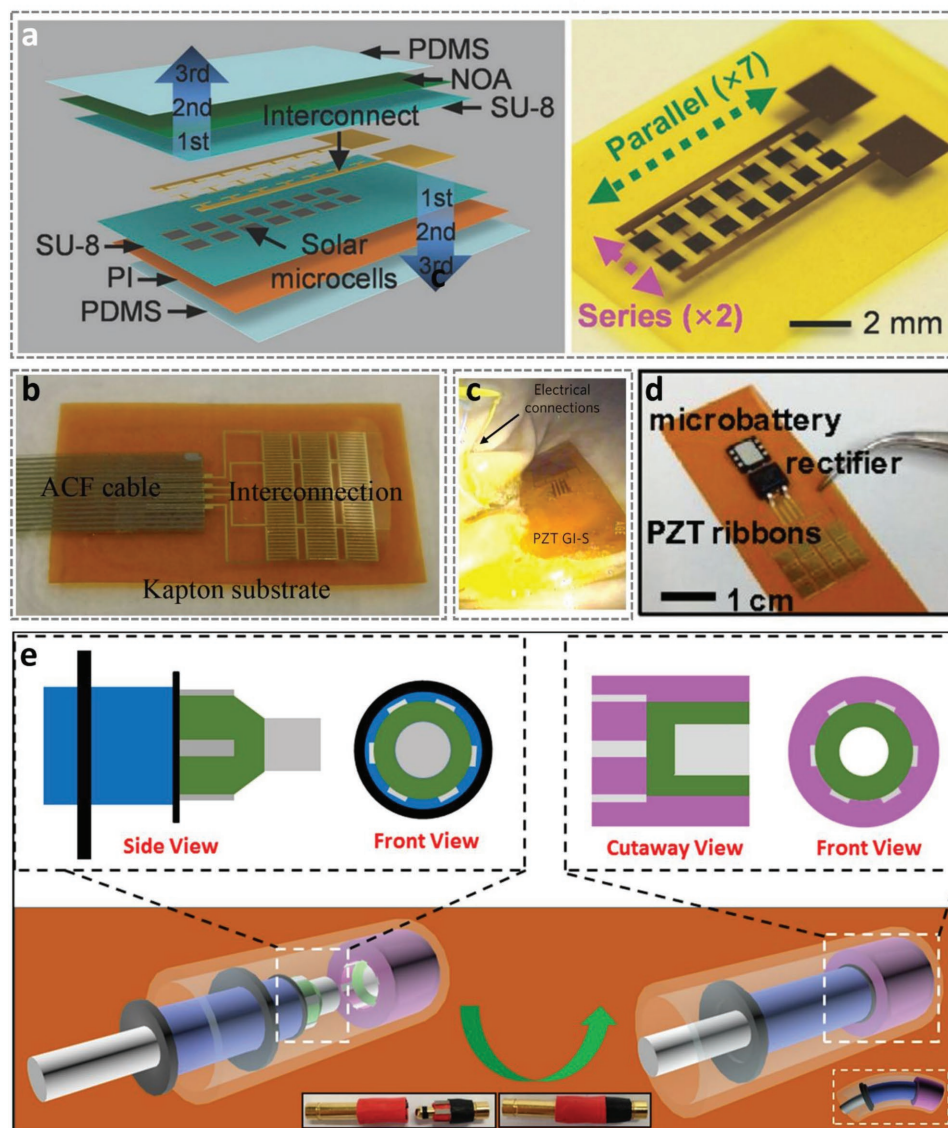


**Figure 10.** Connections of IVEHs. a) A schematic illustration and optical image of structures and connections of micro solar cells. Reproduced with permission.<sup>[15]</sup> Copyright 2016, Wiley-VCH. b) PZT-based IVEH connected with flexible ACF cable. Reproduced with permission.<sup>[6]</sup> Copyright 2015, Springer Nature. c) PZT device on the wall of the stomach. Reproduced with permission.<sup>[71]</sup> Copyright 2017, Springer Nature. d) The photograph of integrated energy harvesting system. Reproduced with permission.<sup>[5]</sup> Copyright 2014, National Academy of Sciences. e) Schematic diagram of the new type of connector for IVEHs. Reproduced with permission.<sup>[50]</sup> Copyright 2016, Wiley-VCH.

generated by the TENG was stored in a temporary capacitor  $C_{temp}$  through a rectifier. At the second stage, the energy of  $C_{temp}$  was transferred to a main energy storage device. The key components of this power management module were two automatic electronic circuits and a coupled inductor. About 90% board efficiency and 60% total efficiency was achieved, which was equal two orders of magnitude better than with direct charging.

2) Powering IMEs directly: Biofuel cells and endocochlear potential cells fall into this category owing to their relatively stable output. Researchers implanted two pairs of biocatalytic electrodes into two lobsters connected in series with electrical wires, which could drive an electronic watch without any intermediate circuits.<sup>[17]</sup>

Although the output of solar cells is steady, some power managing methods are also needed. A 47  $\mu\text{F}$  tantalum capacitor was used as a buffer to power a pacemaker during episodes of temporary energy shortage, such as at night or during the winter. The researchers pointed out that this buffer capacitor was not large enough to run the pacemaker in darkness.<sup>[48]</sup> Rechargeable batteries were used to store the energy generated by implanted photovoltaic devices in rats, which were used to maintain continuous outputs impulses of a pacemaker without light.<sup>[15]</sup>

A significant shortcoming of biofuel cells is the low output voltage, which cannot satisfy the voltage requirements of most IMEs (2–3 V). Therefore, charge pumps and DC–DC converters are often used to enhance the output voltage of biofuel cells.<sup>[41]</sup>

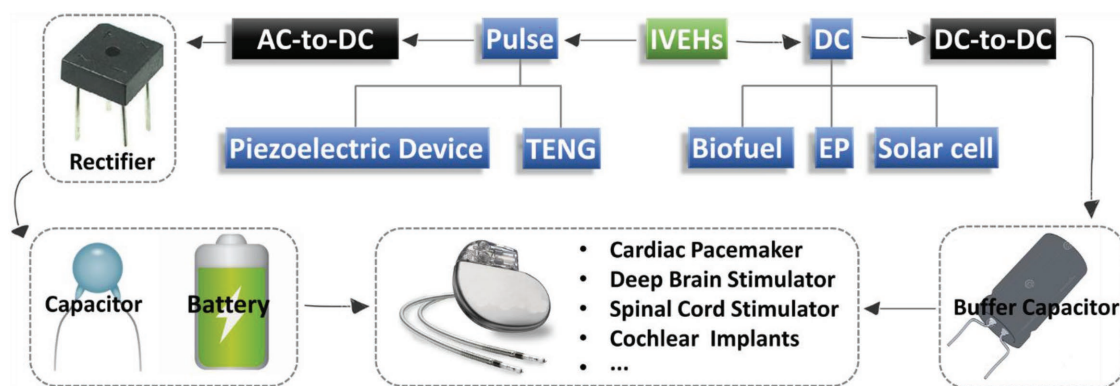


**Figure 11.** Power managements of IVEHs.

For example, three biofuel cells were wired in parallel and connected a 1 F capacitor, which was used to accumulate enough electrical energy to power an electrical motor.<sup>[18]</sup>

#### 4.4. Evaluation Criteria

Suitable standardized evaluations of IVEHs are important for researchers to guide their designs. The evaluation criteria should be primarily related to the following aspects:

- 1) Output properties. These criteria include:  $V_{oc}$ ,  $I_{sc}$ , the current density, power density, maximum output power, internal resistance, energy conversion efficiency, and stability. Zi et al.<sup>[77]</sup> introduced figures-of-merit for quantifying the performance of TENGs in 2015. These values define the performance of TENG devices with regard to their structures and materials that impact the output. Their study may establish some widely accepted standards for practical applications and the industrialization of TENGs.
- 2) In vivo evaluations. Biological safety is among the most important criteria for implantable devices. This includes, device biocompatibility, the safety of the implantation surgery, and long-term durability. Recent evaluations of IVEHs biocompatibility use cellular and tissue responses, by studying whether IVEHs impact cell proliferation or trigger inflammatory reactions. Surgery is an essential process for in vivo applications. The proper surgical strategy is guided by animal models, such as rats, rabbits, pigs, cows, or sheep. Possible implantation sites include the heart, lungs, diaphragm, jugular vein, abdomen of an insect, and hemolymph of molluscs. As an illustration, for a TENG IVEH implanted in pig,<sup>[71]</sup> a typical surgical procedure should include fasting, anesthesia, thoracotomy, and suturing. The long-term durability is directly related with whether the IVEHs can be practicable for clinical applications.
- 3) Clinical criteria. It is likely that IVEHs and IMEs will be used in humans in the future. To date, however, in recent, IVEHs have not been implemented in people, and some experiments using conditions close to the physiological environment of the human body have been performed. Southcott et al.<sup>[78]</sup> assembled a pair of biocatalytic electrodes in a flow biofuel cell filled with a serum solution that mimicked the human circulatory system. This device can generate a  $V_{oc}$

value of about 0.47 V and a  $I_{sc}$  value of about 5 mA. Holade et al.<sup>[79]</sup> created an “abiotic” biofuel cell based on inorganic nanostructured modified catalytic electrodes and a human serum solution. The  $V_{oc}$ , short-circuit current density ( $j_{sc}$ ), and maximum power ( $P_{max}$ ) values in human serum with  $5.4 \times 10^{-3}$  M glucose were 0.35 V, 0.65 mA cm<sup>-2</sup>, and 104  $\mu$ W, respectively. A commercial pacemaker could be powered by storing the generated energy in an on-board 1 mF capacitor. Meanwhile, physical IVEHs, such as piezoelectric and triboelectric devices, have not been tried in humans owing to scientific problems, engineering issues, and medical ethics concerns. Establishing of clinical criteria for IVEHs is challenging but essential. These criteria must correspond with the specifications made by professional organizations, such as CE (Conformité Européenne), FDA (Food and Drug Administration), ISO (International Organization for Standardization), and other regulatory bodies.

#### 4.5. Sensing Applications

IVEHs are not only used as power sources but also as active sensors, especially the physical types. Because the motion of internal organs produces the energy harvested by IVEHs, the outputs of IVEHs are strongly related with many biomedical signals, such as electrocardiogram (ECG), heart rate, blood pressure, velocity of blood flow, and respiratory rate and phase (Figure 12a).

Ma et al.<sup>[22]</sup> presented a self-powered and multifunctional iTEAS, which was used to monitor multiple physiological and pathological signs such as atrial fibrillation and ventricular premature contraction. They implanted the iTEAS into the pericardial sac of a living pig and found that the outputs reflected the properties of heart rate and rhythm, blood pressure, the velocity of blood flow, respiratory rate, and respiratory cycle phase. As a result, a self-powered iTEAS should be able to assist in the real-time diagnosis of heart diseases such as atrial fibrillation, ventricular premature contraction, chronic obstructive pulmonary disease, and asthma (Figure 12b–d).

IVEHs based on the piezoelectric effect are also useful for detecting biological signals. For example, a PMN-PZT energy harvester was used to monitor the hearts of pigs.<sup>[30]</sup> A flexible piezoelectric system based on PZT ribbons was used as a gastrointestinal sensor, which was inserted into a pig

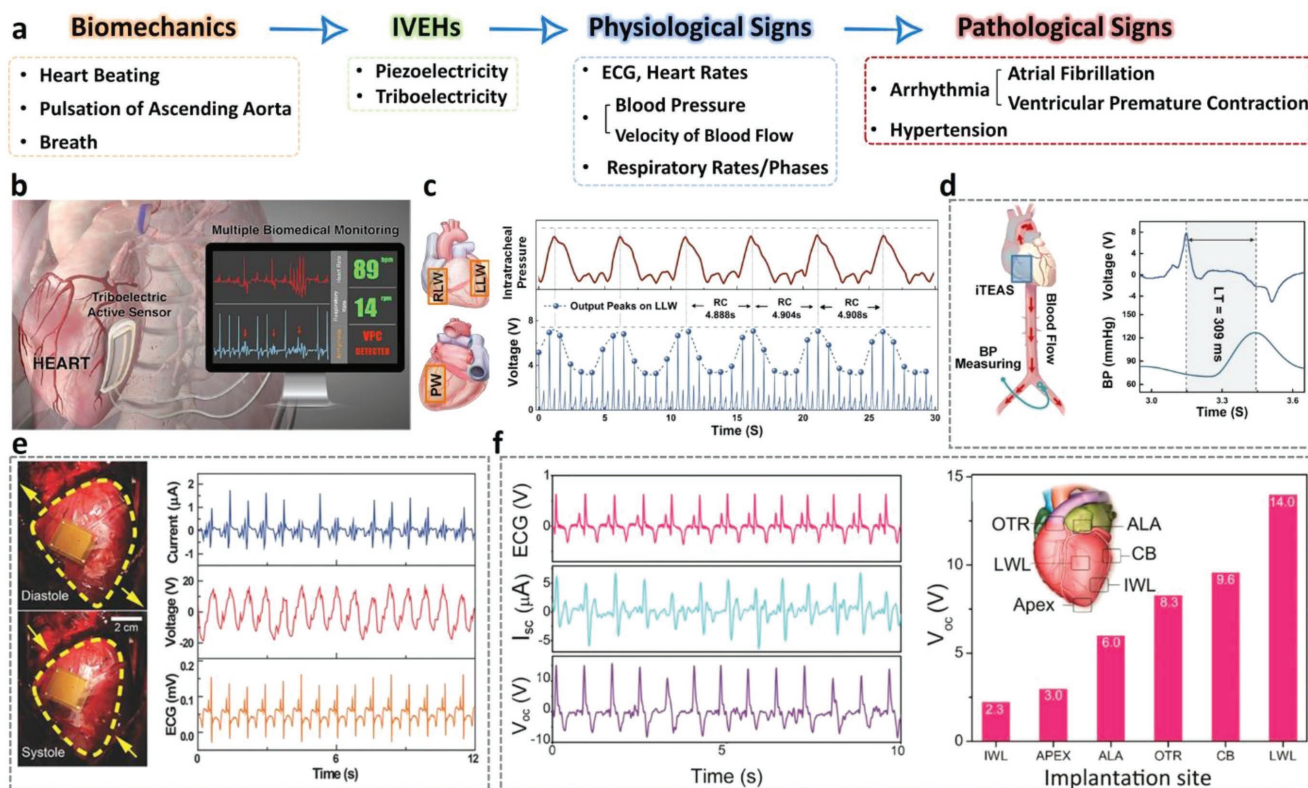


**Figure 12.** a) Schematic diagram of physiological and pathological signs monitored by piezoelectricity and triboelectricity types of IVEHs. b) Schematic diagram of heart monitoring by triboelectric active sensor. c) Peak output voltages of the iTEAS presenting stable periodical fluctuations along with the respiration. d) Monitoring the velocity of blood through iTEAS. Reproduced with permission.<sup>[22]</sup> Copyright 2016, American Chemical Society. e) Left: Photographs of the device when the heart relaxes in diastole and contracts in systole; right: in vivo output open-circuit voltage and short-circuit current of the device derived from porcine heartbeat and simultaneously recorded ECG signals of the pig. Reproduced with permission.<sup>[30]</sup> Copyright 2017, Wiley-VCH. f) Left: in vivo  $V_{oc}$  and  $I_{sc}$  of the iTENG and simultaneously recorded ECG of the swine; right: output of the iTENG at a different implant site (OTR, the right ventricular; ALA, the auricle of the left atrium; CB, the cardiac base; LWL, the lateral wall of the left ventricular; IWL, the inferior wall of the left ventricular). Reproduced with permission.<sup>[8]</sup> Copyright 2016, American Chemical Society.

stomach.<sup>[71]</sup> A PVDF-based piezoelectric thin-film acted as the blood pressure sensor, which was implanted to wrap around ascending aorta of a pig, and could monitor the blood pressure in real time.<sup>[27]</sup> In the future, self-powered active sensors based on IVEHs are expected to be the next-generation of implantable biomedical devices that can monitor multiple physiological and pathological signs, such as ECG, heart rate, respiratory rate and phase, blood pressure, and gastrointestinal signals.

## 5. Conclusions

This review summarized some recent progress in the area of in vivo energy harvesting techniques that have been achieved tested in live models, particularly plants (oranges, grapes, and cacti), insects (cockroaches and moths), molluscs (snails and clams), crustaceans (lobsters), and mammals (rats, rabbits, dogs, pigs, sheep, and cows). IVEHs can be divided into two broad classes: physical—which includes piezoelectric, triboelectric, and automatic wristwatch devices, and chemical—which includes biofuel cells and endocochlear devices. Solar cell IVEHs do not exactly utilize the in vivo bioenergy of livings, but are still important implantable power sources that can harvest optical energy from the ambient environment.

We have discussed IVEHs from the perspective of output properties, fabrication techniques, in vivo experiments, and longevity tests. Meanwhile, their potential uses and the challenges surrounding them have also been presented. Evaluation criteria are urgently needed to qualitatively and quantitatively evaluate the performances of IVEHs, as well as their potential for practical applications and commercialization.

Besides acting as energy harvesting devices, self-powered sensors based on IVEHs can be used for detecting or monitoring physiological signs including ECG, heart rate, blood pressure, velocity of blood flow, respiratory rate and phase, as well as some pathological conditions like atrial fibrillation, ventricular premature contraction, and hypertension. We hope to provide some references for the future study and design of IVEHs and other implanted electronics and systems. In the future, battery-free or self-powered implantable medical electronics are likely to be adopted as a mainstream trend.

## Acknowledgements

This work was supported by the 111 Project (Project No.: B13003), the National Key R & D project from Minister of Science and Technology, China (Grant No. 2016YFA0202703), NSFC (Grant Nos. 31571006, 81601629, and 11421202), Beijing Talents Fund (Grant

No. 2015000021223ZK21), Beijing Natural Science Foundation (2182091) and “Thousands Talents” program for pioneer researcher and his innovation team.

## Conflict of Interest

The authors declare no conflict of interest.

## Keywords

energy harvesting, implantable medical electronics, in vivo, self-powered

Received: March 7, 2018

Revised: April 11, 2018

Published online:

- 
- [1] a) G. T. Hwang, M. Byun, C. K. Jeong, K. J. Lee, *Adv. Healthcare Mater.* **2015**, *4*, 646; b) Q. Zheng, B. Shi, Z. Li, Z. L. Wang, *Adv. Sci. Mater.* **2017**, *4*, 1700029.
- [2] a) E. Talaie, P. Bonnicksen, X. Sun, Q. Pang, X. Liang, L. F. Nazar, *Chem. Mater.* **2016**, *29*, 90; b) R. C. Armstrong, C. Wolfram, K. P. D. Jong, R. Gross, N. S. Lewis, B. Boardman, A. J. Ragauskas, K. Ehrhardt-Martinez, G. Crabtree, M. V. Ramana, *Nat. Energy* **2016**, *1*, 15020.
- [3] A. Pfenniger, M. Jonsson, A. Zurbuchen, V. M. Koch, R. Vogel, *Ann. Biomed. Eng.* **2013**, *41*, 2248.
- [4] Z. Li, G. Zhu, R. Yang, A. C. Wang, Z. L. Wang, *Adv. Mater.* **2010**, *22*, 2534.
- [5] C. Dagdeviren, B. D. Yang, Y. W. Su, P. L. Tran, P. Joe, E. Anderson, J. Xia, V. Doraiswamy, B. Dehdashti, X. Feng, B. W. Lu, R. Poston, Z. Khalpey, R. Ghaffari, Y. G. Huang, M. J. Slepian, J. A. Rogers, *Proc. Natl. Acad. Sci. USA* **2014**, *111*, 1927.
- [6] B. Lu, Y. Chen, D. Ou, H. Chen, L. Diao, W. Zhang, J. Zheng, W. Ma, L. Sun, X. Feng, *Sci. Rep.* **2015**, *5*, 16065.
- [7] F. R. Fan, Z. Q. Tian, Z. L. Wang, *Nano Energy* **2012**, *1*, 328.
- [8] Q. Zheng, H. Zhang, B. Shi, X. Xue, Z. Liu, Y. Jin, Y. Ma, Y. Zou, X. Wang, Z. An, W. Tang, W. Zhang, F. Yang, Y. Liu, X. Lang, Z. Xu, Z. Li, Z. L. Wang, *ACS Nano* **2016**, *10*, 6510.
- [9] Q. Zheng, B. Shi, F. Fan, X. Wang, L. Yan, W. Yuan, S. Wang, H. Liu, Z. Li, Z. L. Wang, *Adv. Mater.* **2014**, *26*, 5851.
- [10] A. Zurbuchen, A. Haeblerlin, A. Pfenniger, L. Bereuter, J. Schaerer, F. Jutzi, C. Huber, J. Fuhrer, R. Vogel, *IEEE Trans. Biomed. Circuits Syst.* **2017**, *11*, 78.
- [11] H. Goto, T. Sugiura, Y. Harada, T. Kazui, *Med. Biol. Eng. Comput.* **1999**, *37*, 377.
- [12] A. Zurbuchen, A. Pfenniger, A. Stahel, C. T. Stoeck, S. Vandenberghe, V. M. Koch, R. Vogel, *Ann. Biomed. Eng.* **2013**, *41*, 131.
- [13] T. Laube, C. Brockmann, R. Buss, C. Lau, K. Höck, N. Stawski, T. Stieglitz, H. A. Richter, H. Schilling, *Graef. Arch. Clin. Exp.* **2004**, *242*, 661.
- [14] A. Haeblerlin, A. Zurbuchen, S. Walpen, J. Schaerer, T. Niederhauser, C. Huber, H. Tanner, H. Servatius, J. Seiler, H. Haeblerlin, J. Fuhrer, R. Vogel, *Heart Rhythm* **2015**, *12*, 1317.
- [15] K. Song, J. H. Han, T. Lim, N. Kim, S. Shin, J. Kim, H. Choo, S. Jeong, Y. C. Kim, Z. L. Wang, *Adv. Healthcare Mater.* **2016**, *5*, 1572.
- [16] E. Katz, K. Macvittie, *Energy Environ. Sci.* **2013**, *6*, 2791.
- [17] K. Macvittie, J. Halamek, L. Halamkova, M. Southcott, W. D. Jemison, R. Lobel, E. Katz, *Energy Environ. Sci.* **2013**, *6*, 81.
- [18] A. Szczupak, J. Halánek, L. Halámková, V. Bocharova, L. Alfonta, E. Katz, *Energy Environ. Sci.* **2012**, *5*, 8891.
- [19] A. Zebda, S. Cosnier, J. P. Alcaraz, M. Holzinger, A. Le Goff, C. Gondran, F. Boucher, F. Giroud, K. Gorgy, H. Lamraoui, P. Cinquin, *Sci. Rep.* **2013**, *3*, 1516.
- [20] S. Yoshino, T. Miyake, T. Yamada, K. Hata, M. Nishizawa, *Adv. Energy Mater.* **2013**, *3*, 60.
- [21] P. P. Mercier, A. C. Lysaght, S. Bandyopadhyay, A. P. Chandrakasan, K. M. Stankovic, *Nat. Biotechnol.* **2012**, *30*, 1240.
- [22] Y. Ma, Q. Zheng, Y. Liu, B. Shi, X. Xue, W. Ji, Z. Liu, Y. Jin, Y. Zou, Z. An, W. Zhang, X. Wang, W. Jiang, Z. Xu, Z. L. Wang, Z. Li, H. Zhang, *Nano Lett.* **2016**, *16*, 6042.
- [23] a) W. Guo, X. Zhang, X. Yu, S. Wang, J. Qiu, W. Tang, L. Li, H. Liu, Z. L. Wang, *ACS Nano* **2016**, *10*, 5086; b) G. T. Hwang, H. Park, J. H. Lee, S. Oh, K. I. Park, M. Byun, H. Park, G. Ahn, C. K. Jeong, K. No, *Adv. Mater.* **2014**, *26*, 4880; c) G. Zhu, A. C. Wang, Y. Liu, Y. Zhou, Z. L. Wang, *Nano Lett.* **2012**, *12*, 3086; d) W. Tang, J. Tian, Q. Zheng, L. Yan, J. Wang, Z. Li, Z. L. Wang, *ACS Nano* **2015**, *9*, 7867; e) Y. Jin, J. Seo, J. S. Lee, S. Shin, H. J. Park, S. Min, E. Cheong, T. Lee, S. W. Cho, *Adv. Mater.* **2016**, *28*, 7293.
- [24] Q. Zheng, Y. Zou, Y. Zhang, Z. Liu, B. Shi, X. Wang, Y. Jin, H. Ouyang, Z. Li, Z. L. Wang, *Sci. Adv.* **2016**, *2*, e1501478.
- [25] Z. L. Wang, J. Song, *Science* **2006**, *312*, 242.
- [26] H. Zhang, X.-S. Zhang, X. Cheng, Y. Liu, M. Han, X. Xue, S. Wang, F. Yang, S. A. S. H. Zhang, Z. Xu, *Nano Energy* **2015**, *12*, 296.
- [27] X. Cheng, X. Xue, Y. Ma, M. Han, W. Zhang, Z. Xu, H. Zhang, H. Zhang, *Nano Energy* **2016**, *22*, 453.
- [28] Y. Yu, H. Sun, H. Orbay, C. Feng, C. G. England, W. Cai, X. Wang, *Nano Energy* **2016**, *27*, 275.
- [29] C. K. Jeong, J. H. Han, H. Palneedi, H. Park, G. T. Hwang, B. Joung, S. G. Kim, H. J. Shin, I. S. Kang, J. Ryu, K. J. Lee, *Appl. Mater.* **2017**, *5*, 074102.
- [30] D. H. Kim, H. J. Shin, H. Lee, C. K. Jeong, H. Park, G. T. Hwang, H. Y. Lee, D. J. Joe, J. H. Han, S. H. Lee, J. Kim, B. Joung, K. J. Lee, *Adv. Funct. Mater.* **2017**, *27*, 1700341.
- [31] A. Wang, Z. Liu, M. Hu, C. Wang, X. Zhang, B. Shi, Y. Fan, Y. Cui, Z. Li, K. Ren, *Nano Energy* **2018**, *43*, 63.
- [32] a) J. Tian, H. Feng, L. Yan, M. Yu, H. Ouyang, H. Li, W. Jiang, Y. Jin, G. Zhu, Z. Li, *Nano Energy* **2017**, *36*, 241; b) H. Ouyang, J. Tian, G. Sun, Y. Zou, Z. Liu, H. Li, L. Zhao, B. Shi, Y. Fan, Y. Fan, Z. L. Wang, Z. Li, *Adv. Mater.* **2017**, *29*, 1703456.
- [33] Z. L. Wang, *ACS Nano* **2013**, *7*, 9533.
- [34] M. B. Majewski, A. J. Howarth, P. Li, M. R. Wasielewski, J. T. Hupp, O. K. Farha, *CrystEngComm* **2017**, *19*, 4082.
- [35] U. Schröder, *Angew. Chem.* **2012**, *51*, 7370.
- [36] V. Flexer, N. Mano, *Anal. Chem.* **2010**, *82*, 1444.
- [37] T. Miyake, K. Haneda, N. Nagai, Y. Yatagawa, H. Onami, S. Yoshino, T. Abe, M. Nishizawa, *Energy Environ. Sci.* **2011**, *4*, 5008.
- [38] K. Macvittie, T. Conlon, E. Katz, *Bioelectrochemistry* **2015**, *106*, 28.
- [39] P. Cinquin, C. Gondran, F. Giroud, S. Mazabrard, A. Pellissier, F. Boucher, J. P. Alcaraz, K. Gorgy, F. Lenouvel, S. Mathé, P. Porcu, S. Cosnier, *PLoS One* **2010**, *5*, e10476.
- [40] S. El Ichi, A. Zebda, J. P. Alcaraz, A. Laaroussi, F. Boucher, J. Boutonnat, N. Reverdy-Bruas, D. Chaussy, M. N. Belgacem, P. Cinquin, D. K. Martin, *Energy Environ. Sci.* **2015**, *8*, 1017.
- [41] J. A. Castorena-Gonzalez, C. Foote, K. Macvittie, J. Halánek, L. Halámková, L. A. Martinez-Lemus, E. Katz, *Electroanalysis* **2013**, *25*, 1579.
- [42] L. Halámková, J. Halánek, V. Bocharova, A. Szczupak, L. Alfonta, E. Katz, *J. Am. Chem. Soc.* **2012**, *134*, 5040.
- [43] J. Schwefel, R. E. Ritzmann, I. N. Lee, A. Pollack, W. Weeman, S. Garverick, M. Willis, M. Rasmussen, D. Scherson, *J. Electrochem. Soc.* **2014**, *161*, H3113.
- [44] M. Rasmussen, R. E. Ritzmann, I. Lee, A. J. Pollack, D. Scherson, *J. Am. Chem. Soc.* **2012**, *134*, 1458.
- [45] K. Shoji, Y. Akiyama, M. Suzuki, N. Nakamura, H. Ohno, K. Morishima, *Biosens. Bioelectron.* **2016**, *78*, 390.

- [46] F. C. P. F. Sales, R. M. Iost, M. V. A. Martins, M. C. Almeida, F. N. Crespilho, *Lab Chip* **2013**, *13*, 468.
- [47] P. Nadeau, D. El-Damak, D. Glettig, Y. L. Kong, S. Mo, C. Cleveland, L. Booth, N. Roxhed, R. Langer, A. P. Chandrakasan, G. Traverso, *Nat. Biomed. Eng.* **2017**, *1*, 0022.
- [48] A. Haebler, A. Zurbuchen, J. Schaerer, J. Wagner, S. Walpen, C. Huber, H. Haebler, J. Fuhrer, R. Vogel, *Europace* **2014**, *16*, 1534.
- [49] a) K. Y. Lee, M. K. Gupta, S. W. Kim, *Nano Energy* **2015**, *14*, 139; b) W. S. Jung, M. G. Kang, H. G. Moon, S. H. Baek, S. J. Yoon, Z. L. Wang, S. W. Kim, C. Y. Kang, *Sci. Rep.* **2015**, *5*, 9309; c) G. Wang, Y. Xi, H. Xuan, R. Liu, X. Chen, L. Cheng, *Nano Energy* **2015**, *18*, 28.
- [50] B. J. Shi, Q. Zheng, W. Jiang, L. Yan, X. X. Wang, H. Liu, Y. Yao, Z. Li, Z. L. Wang, *Adv. Mater.* **2016**, *28*, 846.
- [51] a) B. Yang, C. Lee, W. L. Kee, S. P. Lim, *J. Micro-Nanolithogr. MEMS, MOEMS* **2010**, *9*, 023002; b) A. Khaligh, P. Zeng, C. Zheng, *IEEE Trans. Ind. Electron.* **2010**, *57*, 850; c) Z. L. Xu, X. X. Wang, X. B. Shan, T. Xie, *Adv. Mater. Des. Mech.* **2012**, *569*, 529; d) M. Ibrahim, A. Salehian, *J. Intell. Mater. Syst. Struct.* **2015**, *26*, 1259.
- [52] a) B. Kumar, S. W. Kim, *Nano Energy* **2012**, *1*, 342; b) D. Choi, K. Y. Lee, M. J. Jin, S. G. Ihn, S. Yun, X. Bulliard, W. Choi, S. Y. Lee, S. W. Kim, J. Y. Choi, J. M. Kim, Z. L. Wang, *Energy Environ. Sci.* **2011**, *4*, 4607; c) G. C. Yoon, K. S. Shin, M. K. Gupta, K. Y. Lee, J. H. Lee, Z. L. Wang, S. W. Kim, *Nano Energy* **2015**, *12*, 547; d) M. Lee, R. Yang, C. Li, Z. L. Wang, *J. Phys. Chem. Lett.* **2010**, *1*, 2929; e) C. Xu, X. D. Wang, Z. L. Wang, *J. Am. Chem. Soc.* **2009**, *131*, 5866; f) C. F. Tan, W. L. Ong, G. W. Ho, *ACS Nano* **2015**, *9*, 7661.
- [53] a) S. Lee, S. H. Bae, L. Lin, S. Ahn, C. Park, S. W. Kim, S. N. Cha, Y. J. Park, Z. L. Wang, *Nano Energy* **2013**, *2*, 817; b) J. H. Lee, K. Y. Lee, M. K. Gupta, T. Y. Kim, D. Y. Lee, J. Oh, C. Ryu, W. J. Yoo, C. Y. Kang, S. J. Yoon, J. B. Yoo, S. W. Kim, *Adv. Mater.* **2014**, *26*, 765.
- [54] P. Gambier, S. R. Anton, N. Kong, A. Erturk, D. J. Inman, *Meas. Sci. Technol.* **2012**, *23*, 015101.
- [55] B. J. Hansen, Y. Liu, R. S. Yang, Z. L. Wang, *ACS Nano* **2010**, *4*, 3647.
- [56] a) K. W. Zhang, X. Wang, Y. Yang, Z. L. Wang, *ACS Nano* **2015**, *9*, 3521.; b) Y. F. Hu, J. Yang, S. M. Niu, W. Z. Wu, Z. L. Wang, *ACS Nano* **2014**, *8*, 7442.; c) T. Quan, X. Wang, Z. L. Wang, Y. Yang, *ACS Nano* **2015**, *9*, 12301.
- [57] Y. Yang, H. L. Zhang, J. Chen, S. M. Lee, T. C. Hou, Z. L. Wang, *Energy Environ. Sci.* **2013**, *6*, 1744.
- [58] a) S. B. Jeon, D. Kim, G. W. Yoon, J. B. Yoon, Y. K. Choi, *Nano Energy* **2015**, *12*, 636; b) Y. Yang, H. L. Zhang, Y. Liu, Z. H. Lin, S. Lee, Z. Y. Lin, C. P. Wong, Z. L. Wang, *ACS Nano* **2013**, *7*, 2808.
- [59] a) Y. Yang, H. L. Zhang, Z. H. Lin, Y. Liu, J. Chen, Z. Y. Lin, Y. S. Zhou, C. P. Wong, Z. L. Wang, *Energy Environ. Sci.* **2013**, *6*, 2429; b) Y. C. Wu, X. D. Zhong, X. Wang, Y. Yang, Z. L. Wang, *Nano Res.* **2014**, *7*, 1631; c) J. Kim, J. H. Lee, H. Ryu, J. H. Lee, U. Khan, K. Han, S. S. Kwak, S. W. Kim, *Adv. Funct. Mater.* **2017**, *27*, 1700702.
- [60] Y. L. Zi, L. Lin, J. Wang, S. H. Wang, J. Chen, X. Fan, P. K. Yang, F. Yi, Z. L. Wang, *Adv. Mater.* **2015**, *27*, 2340.
- [61] a) N. Wang, L. Han, H. C. He, N. H. Park, K. Koumoto, *Energy Environ. Sci.* **2011**, *4*, 3676; b) T. J. Hsueh, J. M. Shieh, Y. M. Yeh, *Prog. Photovoltaics* **2015**, *23*, 507; c) Y. J. Zhang, J. Fang, C. He, H. Yan, Z. X. Wei, Y. F. Li, *J. Phys. Chem. C* **2013**, *117*, 24685; d) T. Park, J. Na, B. Kim, Y. Kim, H. Shin, E. Kim, *ACS Nano* **2015**, *9*, 11830.
- [62] a) L. Zhang, S. Bai, C. Su, Y. B. Zheng, Y. Qin, C. Xu, Z. L. Wang, *Adv. Funct. Mater.* **2015**, *25*, 5794; b) Y. Qin, X. D. Wang, Z. L. Wang, *Nature* **2008**, *451*, 809.
- [63] N. R. Alluri, B. Saravanakumar, S. J. Kim, *ACS Appl. Mater. Interfaces* **2015**, *7*, 9831.
- [64] M. Lee, C. Y. Chen, S. Wang, S. N. Cha, Y. J. Park, J. M. Kim, L. J. Chou, Z. L. Wang, *Adv. Mater.* **2012**, *24*, 1759.
- [65] M. Zhang, T. Gao, J. S. Wang, J. J. Liao, Y. Q. Qiu, Q. Yang, H. Xue, Z. Shi, Y. Zhao, Z. X. Xiong, L. F. Chen, *Nano Energy* **2015**, *13*, 298.
- [66] M. M. Alam, S. K. Ghosh, A. Sultana, D. Mandal, *Nanotechnology* **2015**, *26*, 165403.
- [67] K. Y. Lee, D. Kim, J. H. Lee, T. Y. Kim, M. K. Gupta, S. W. Kim, *Adv. Funct. Mater.* **2014**, *24*, 37.
- [68] Z. Y. Zhan, L. X. Zheng, Y. Z. Pan, G. Z. Sun, L. Li, *J. Mater. Chem.* **2012**, *22*, 2589.
- [69] Q. L. Liao, Z. Zhang, X. H. Zhang, M. Mohr, Y. Zhang, H. J. Fecht, *Nano Res.* **2014**, *7*, 917.
- [70] S. H. Wu, L. D. Du, D. Y. Kong, H. Y. Ping, Z. Fang, Z. Zhao, *Chin. Phys. B* **2014**, *23*, 044302.
- [71] C. Dagdeviren, F. Javid, P. Joe, T. V. Erlach, T. Bense, Z. Wei, S. Saxton, C. Cleveland, L. Booth, S. McDonnell, J. Collins, A. Hayward, R. Langer, G. Traverso, *Nat. Biomed. Eng.* **2017**, *1*, 807.
- [72] Y. H. Joung, *Int. Neurolog. J.* **2013**, *17*, 98.
- [73] Q. Zheng, Y. M. Jin, Z. Liu, H. Ouyang, H. Li, B. J. Shi, W. Jiang, H. Zhang, Z. Li, Z. L. Wang, *ACS Appl. Mater. Interfaces* **2016**, *8*, 26697.
- [74] M. M. Yuan, L. Cheng, Q. Xu, W. W. Wu, S. Bai, L. Gu, Z. Wang, J. Lu, H. P. Li, Y. Qin, T. Jing, Z. L. Wang, *Adv. Mater.* **2014**, *26*, 7432.
- [75] H. Heinilä, J. Riistama, P. Heino, J. Lekkala, *Circuit World* **2009**, *35*, 34.
- [76] S. M. Niu, X. F. Wang, F. Yi, Y. S. Zhou, Z. L. Wang, *Nat. Commun.* **2015**, *6*, 8975.
- [77] Y. L. Zi, S. M. Niu, J. Wang, Z. Wen, W. Tang, Z. L. Wang, *Nat. Commun.* **2015**, *6*, 8376.
- [78] M. Southcott, K. Macvittie, J. Halámek, L. Halámková, W. D. Jemison, R. Lobel, E. Katz, *Phys. Chem. Chem. Phys.* **2013**, *15*, 6278.
- [79] Y. Holade, K. MacVittie, T. Conlon, N. Guz, K. Servat, T. W. Napporn, K. B. Kokoh, E. Katz, *Electroanalysis* **2014**, *26*, 2445.